

# Connection of electron and phonon structure of scintillators with spatial structure of excited regions and efficiency of bulk and nano scintillators

A.N.Vasil'ev

Skobeltsyn Institute of Nuclear Physics,  
Lomonosov Moscow State University

[anvasiliev@rambler.ru](mailto:anvasiliev@rambler.ru)

# Cascade

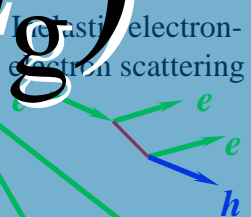
# Transport

# Center

$$(\beta E_g)^{-1}$$

# S

# Q



Thermalization of electrons

Creation of excitons, capture of electrons and holes by different

CONDUCTION BAND

Interaction of excitations  
 $c^* + c^* \rightarrow c + c^*$

Emission  
 $c^* \rightarrow c + h\nu$

$ex + ex \rightarrow ex$

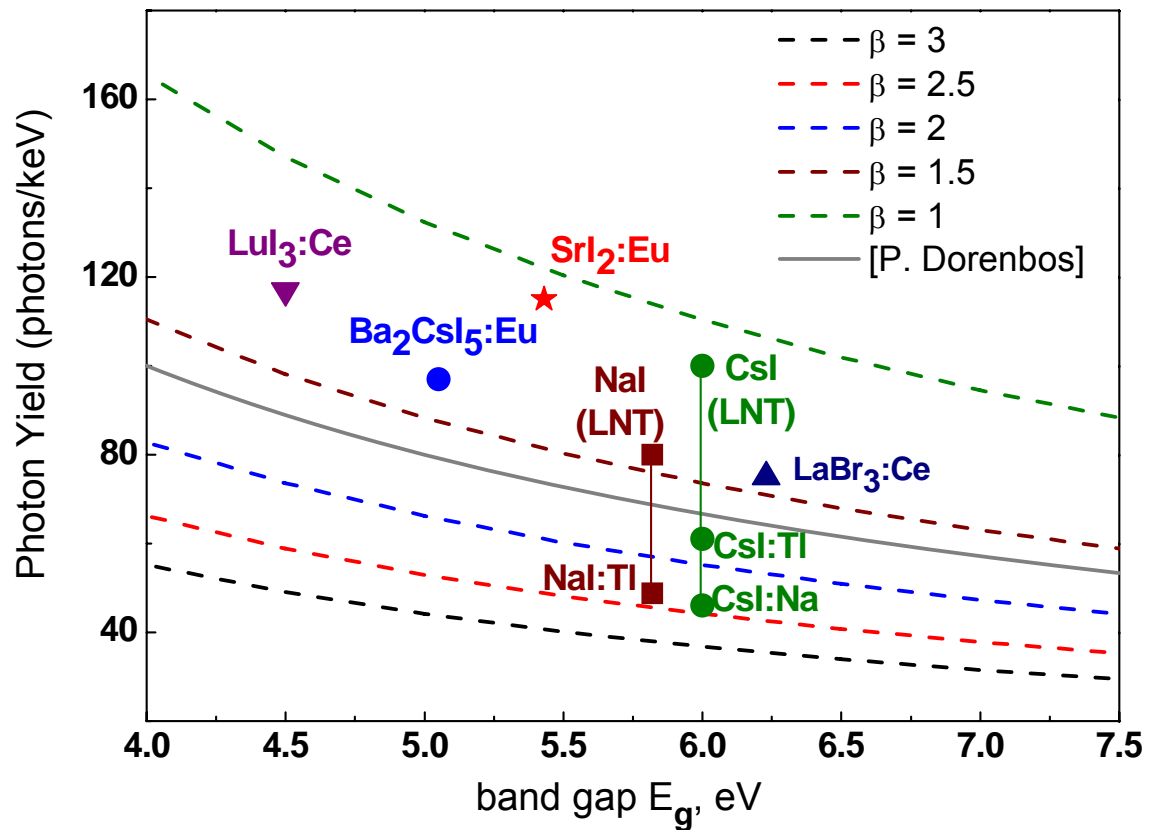
VALENCE BAND

CORE BAND

$10^{-10}$   
sec

$10^{-8}$  sec

$t$



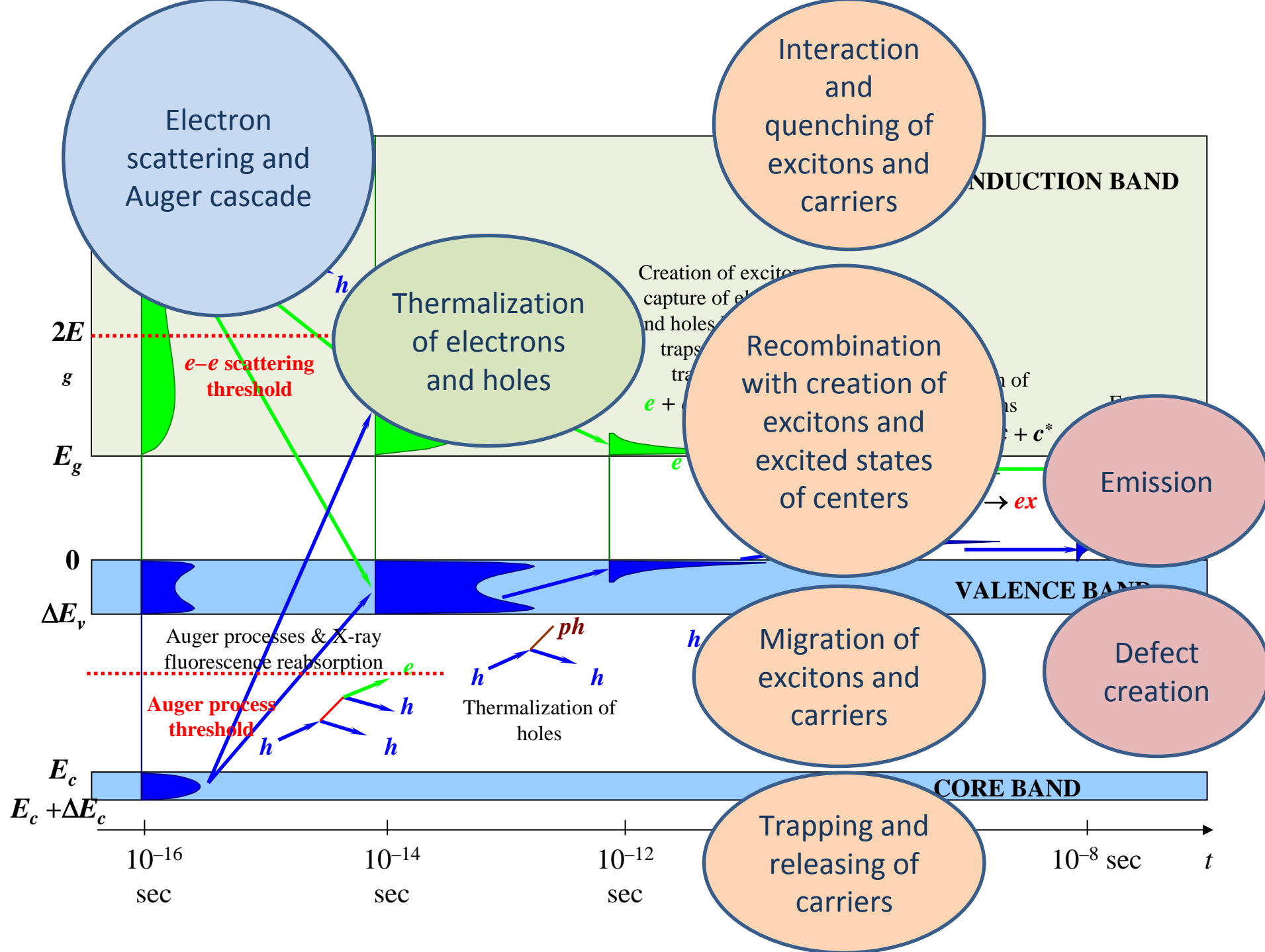
Applications and material engineering request quantitative predictions of properties of new scintillating materials

Simple estimation of scintillation efficiency as  $\beta SQ$  (cascade-transport-center) is only qualitative

~~New theory of scintillations?~~

Re-estimation of the role of different stages of energy relaxation in crystals on the basis of deeper experimental investigation of new materials

Contemporary model: Scintillation as collective interconnected processes of spatial and temporal evolution of strongly non-equilibrium excited region in media



Electron scattering and Auger cascade

Thermalization of electrons and holes

Interaction and quenching of excitons and carriers

Recombination with creation of excitons and excited states of centers

Migration of excitons and carriers

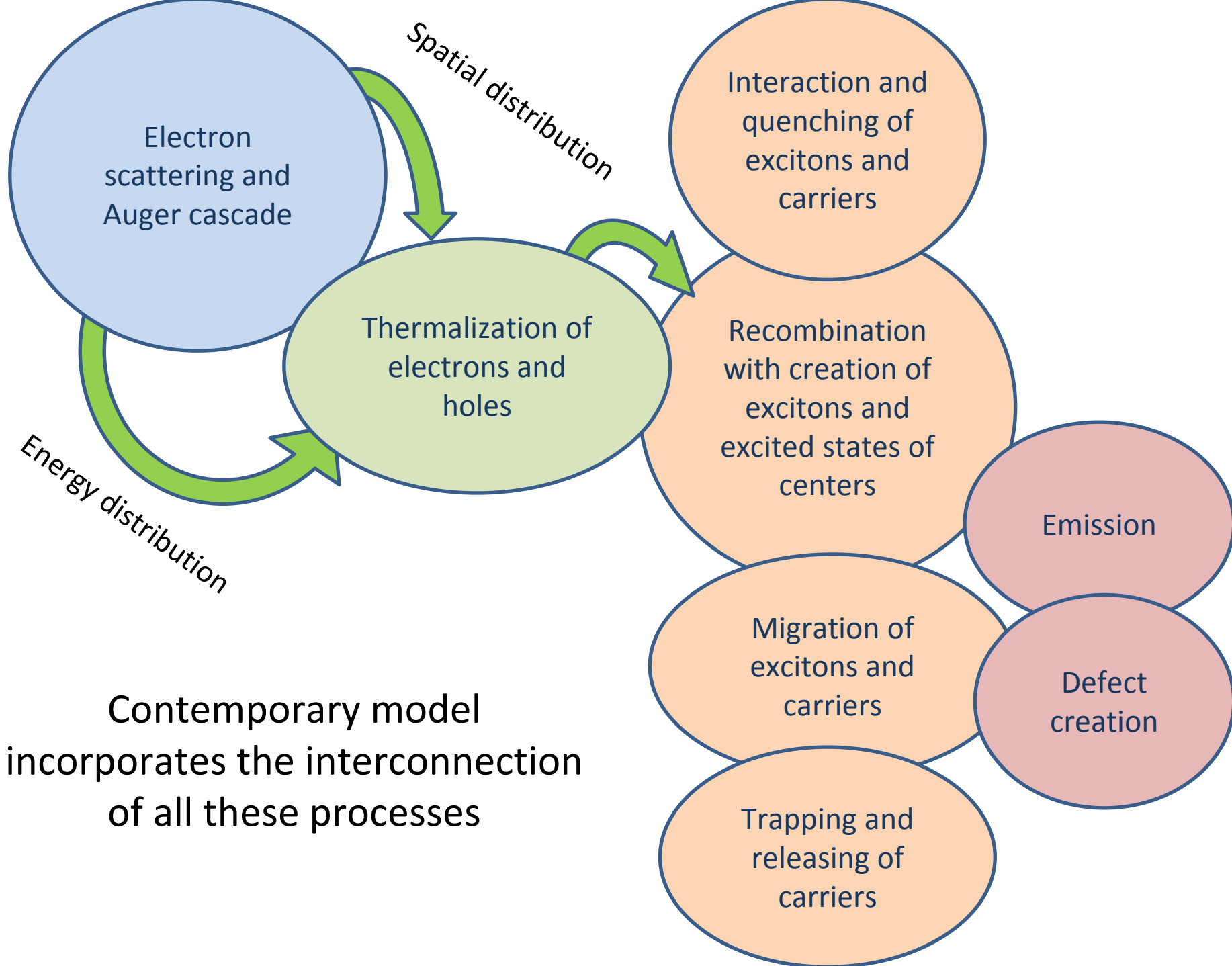
Trapping and releasing of carriers

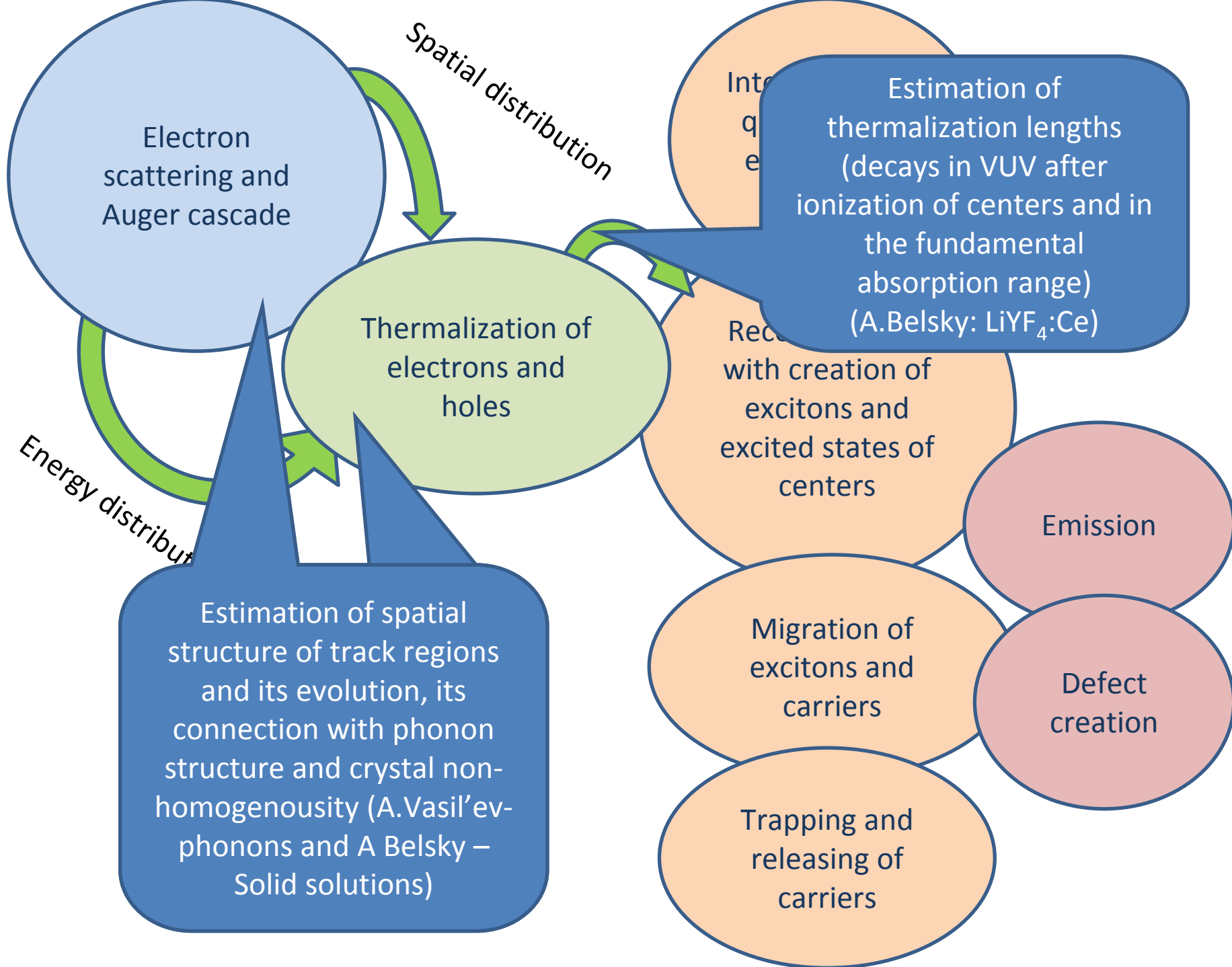
Emission

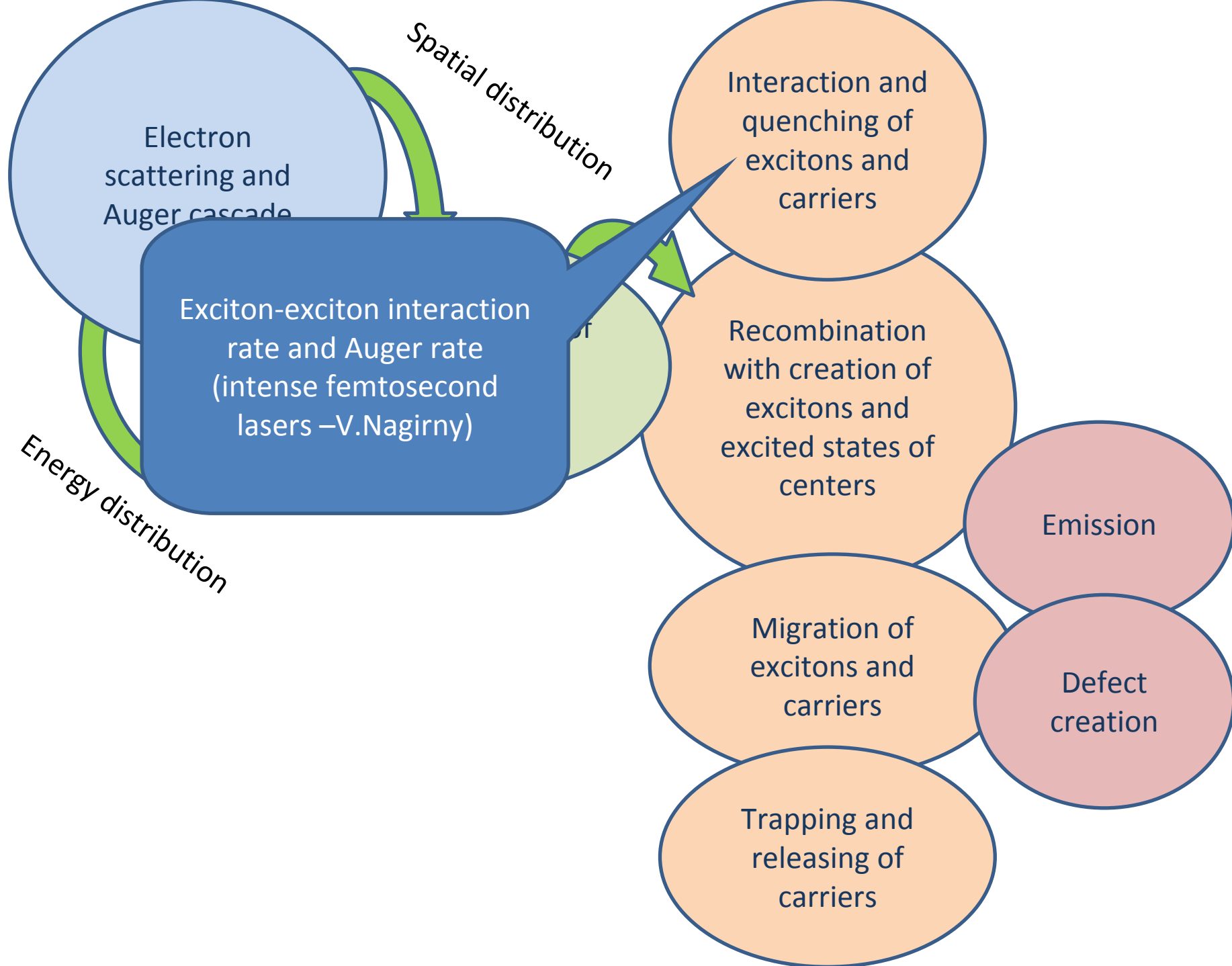
Defect creation

Are these processes independent?

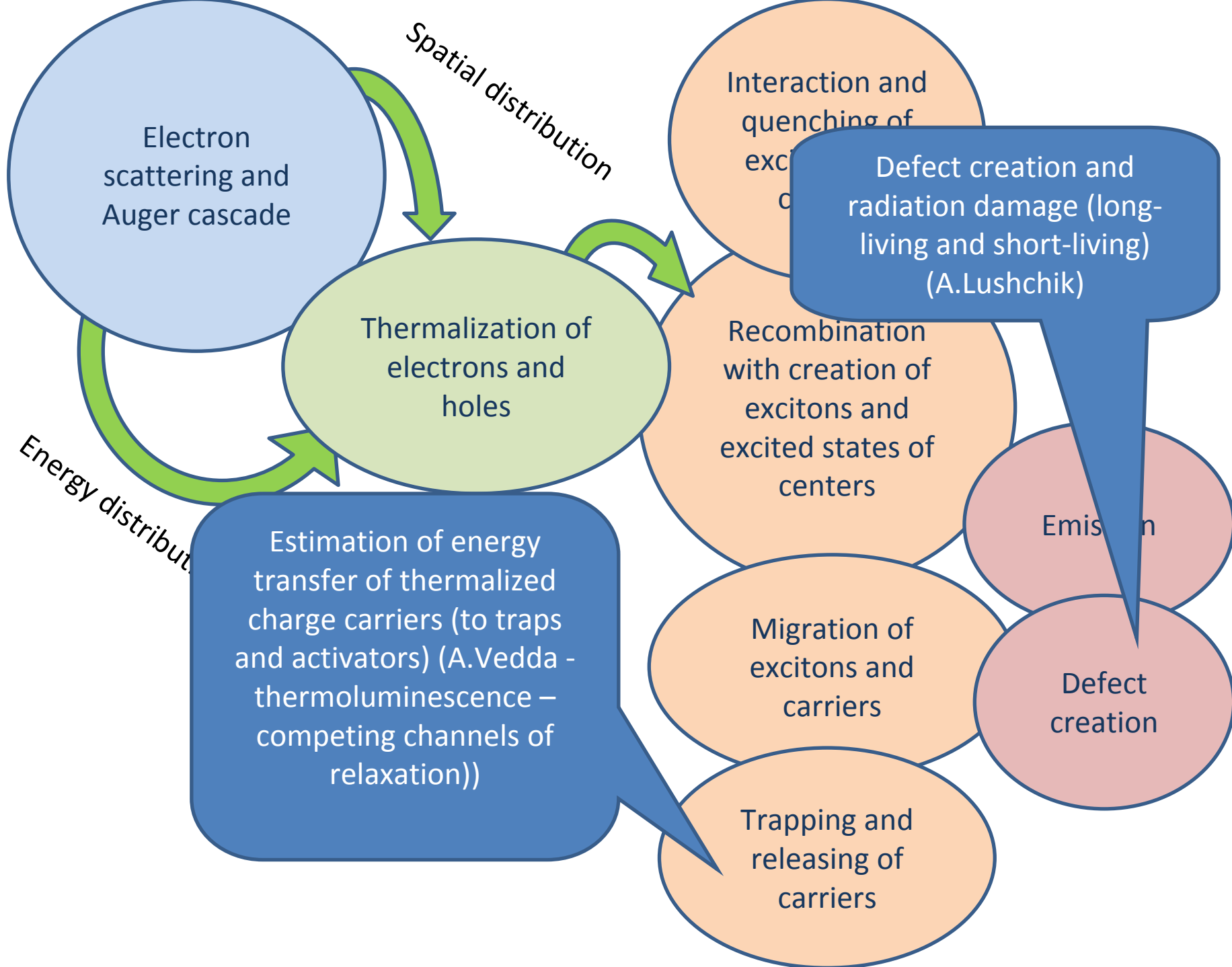
**NO!**

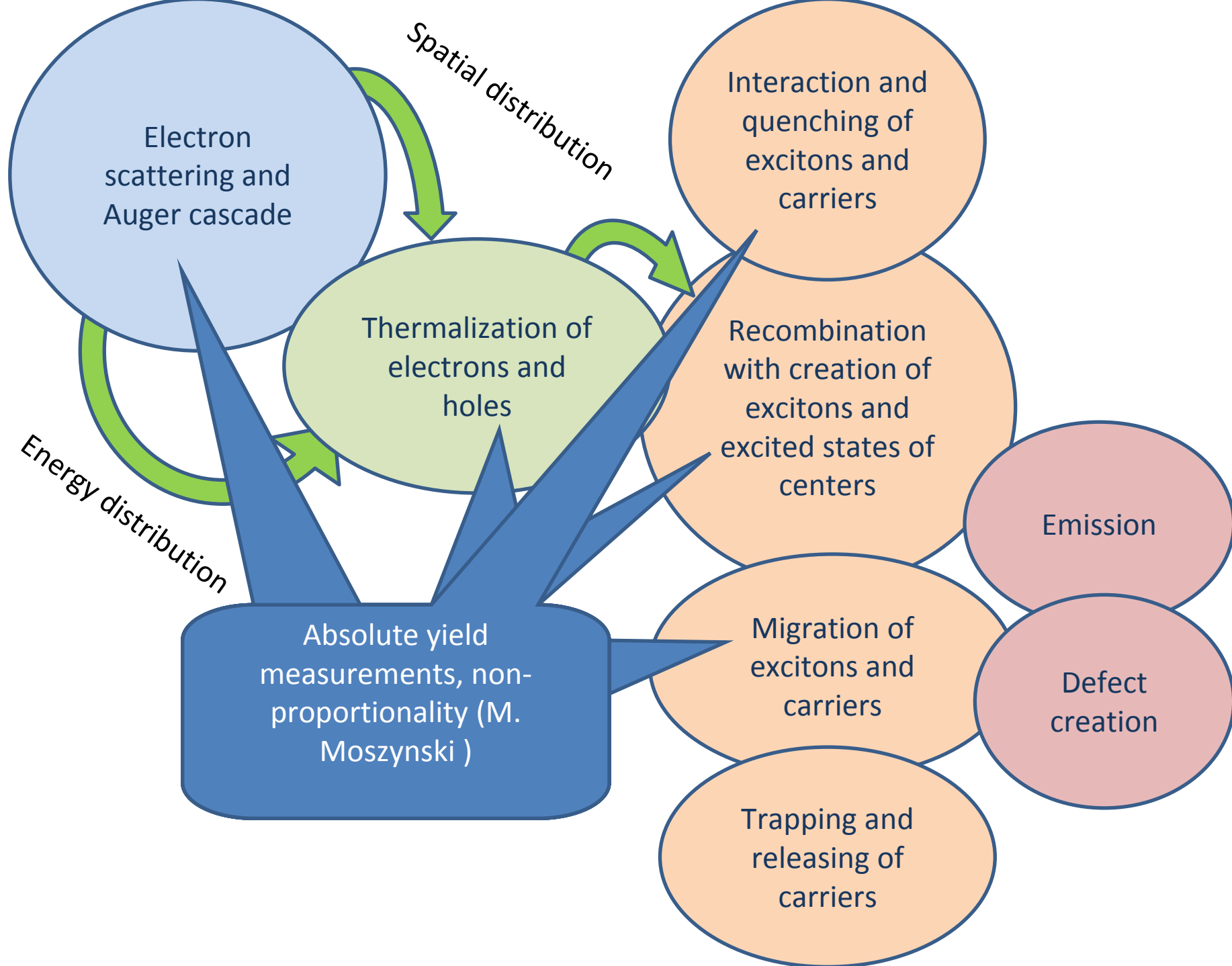












Electron scattering and Auger cascade

Spatial distribution

Interaction and quenching of excitons and carriers

Thermalization of electrons and holes

Recombination with creation of excitons and excited states of centers

Energy distribution

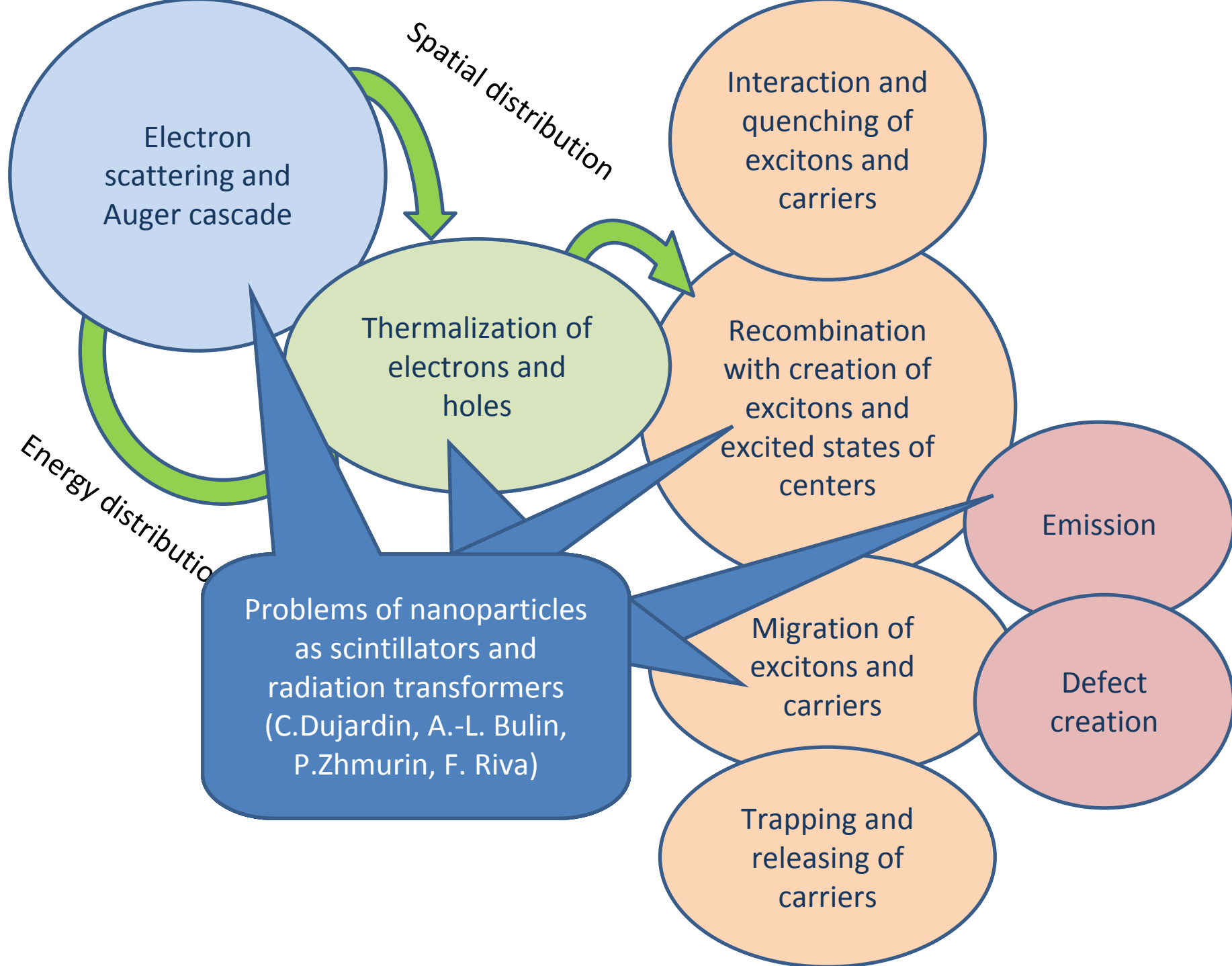
Emission

Absolute yield measurements, non-proportionality (M. Moszynski)

Migration of excitons and carriers

Defect creation

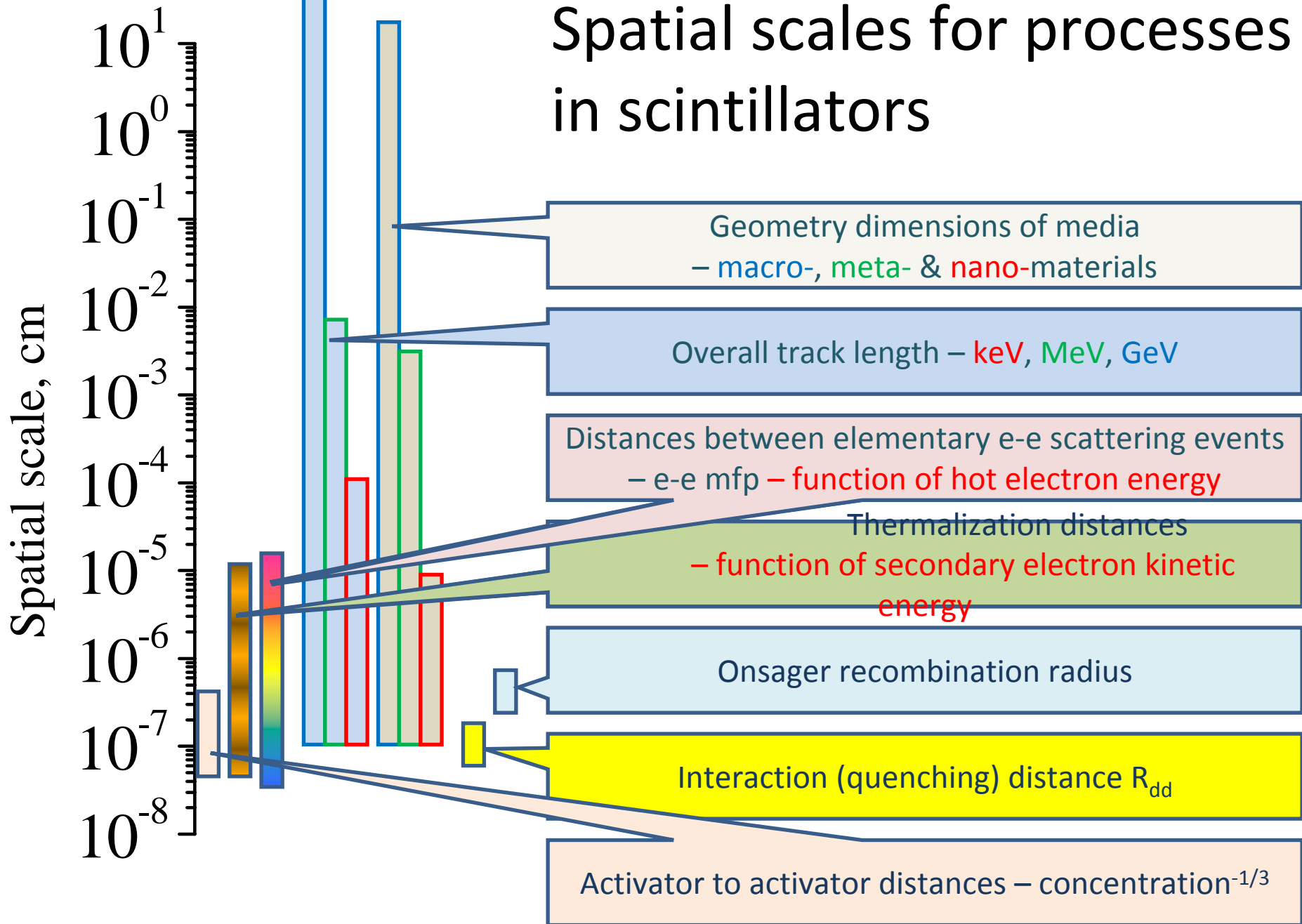
Trapping and releasing of carriers



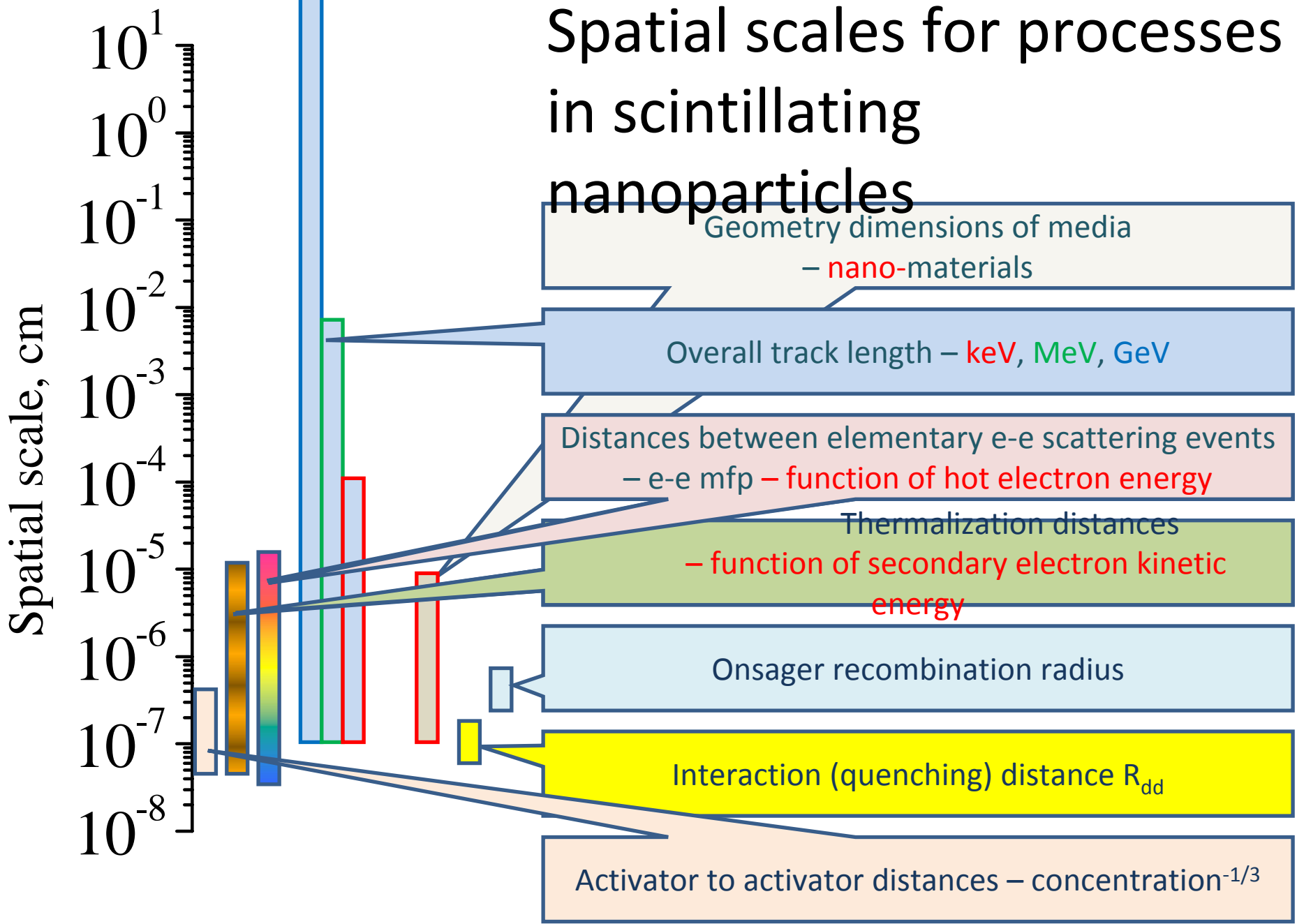
# Outline

- Spatial scales for processes in scintillators
- Nanoparticles as scintillators
- Cascade, thermalization and recombination
- Different types of mobilities
- Thermalization length for different types of crystals
- Interconnection of cascade, thermalization and recombination stages in binary iodides
- Why cascade is so effective in CsI?
- Thermalization length and impurities
- Concluding remarks

# Spatial scales for processes in scintillators

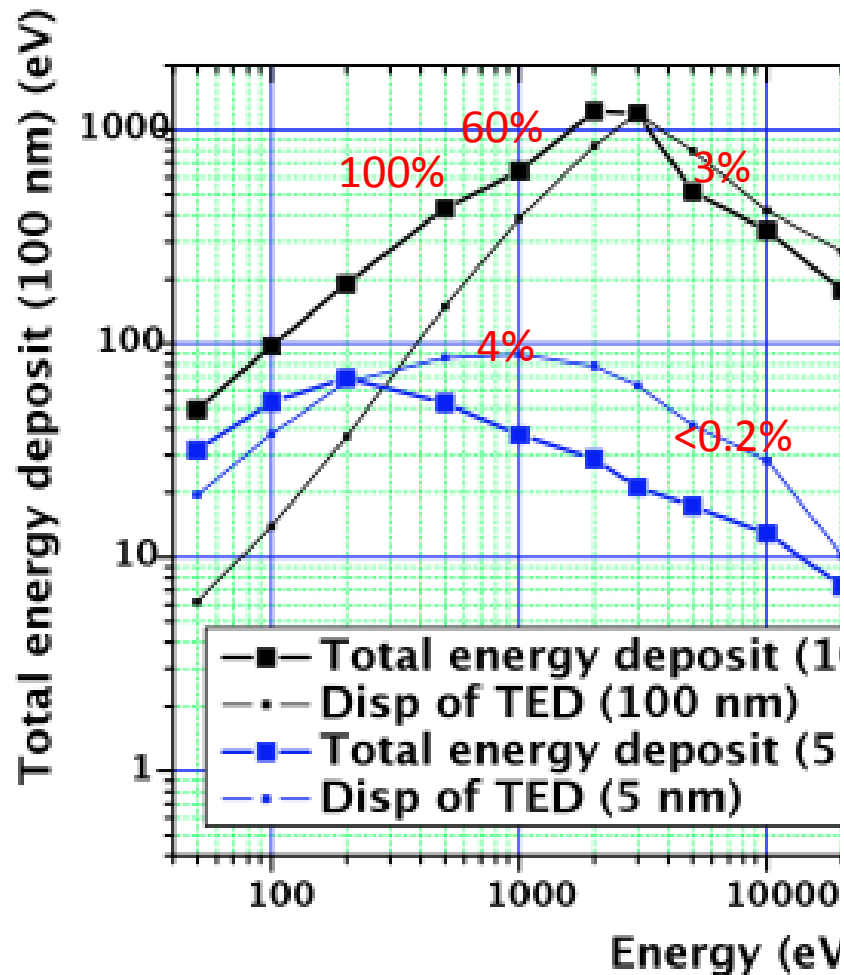


# Spatial scales for processes in scintillating nanoparticles



# Energy deposited within nanoparticles

Total energy deposited as a function of the energy of the primary electron



Vistovskyy *et al.* J. Appl. Phys. 112, 024325 (2012)

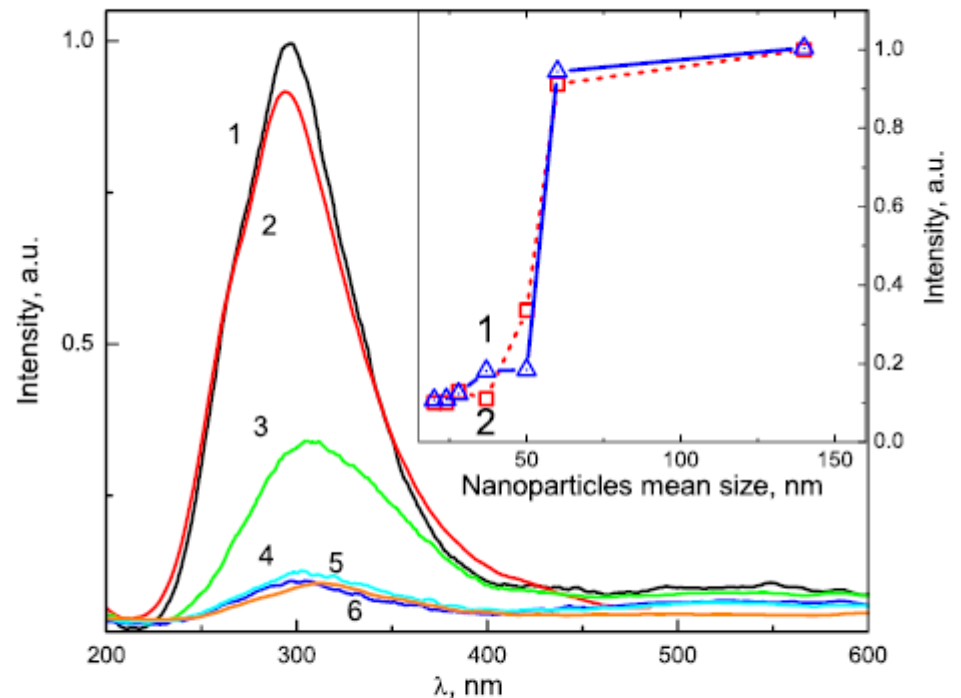
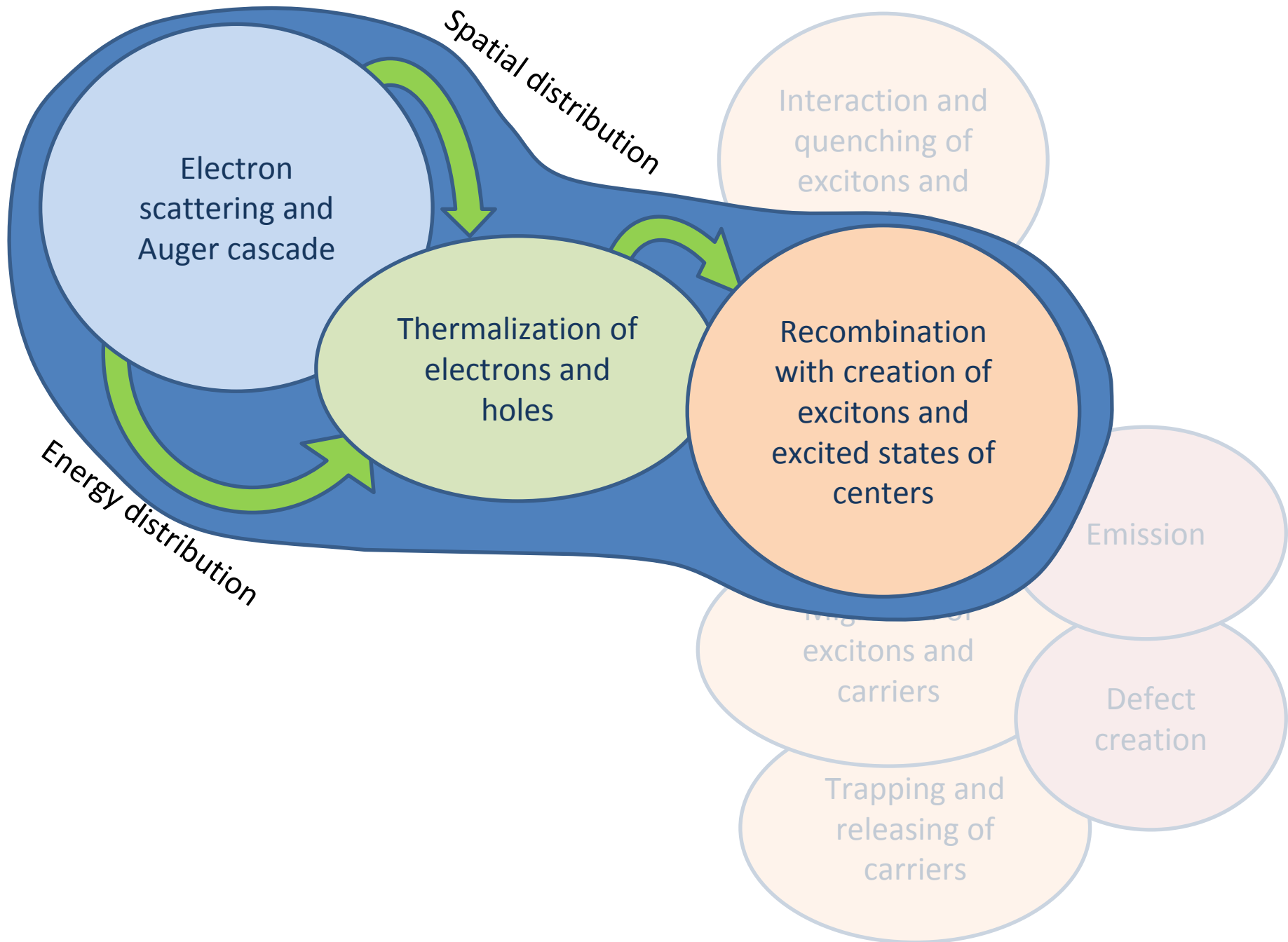


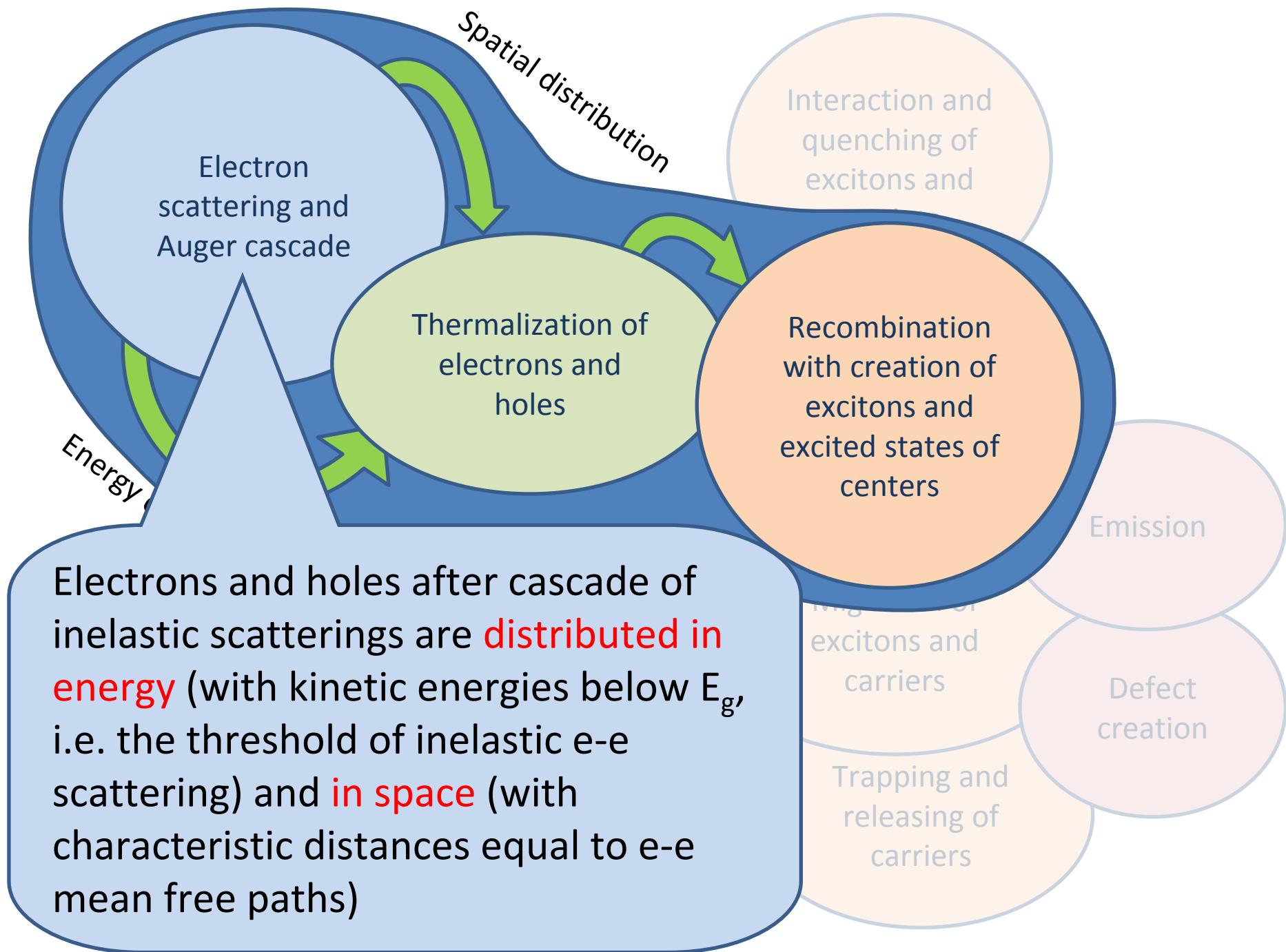
FIG. 6. X-ray excited luminescence spectra of  $\text{CaF}_2$  nanoparticles of various size at 300K. Curves: 1–140; 2–60; 3–50; 4–37; 5–28; 6–20 nm. The dependence of normalized luminescence intensity on the nanoparticle size is shown on inset: curve 1—luminescence intensity upon the excitation by quanta with energy  $h\nu_{\text{exc}} = 16\text{eV}$ , curve 2—X-ray excited luminescence intensity.

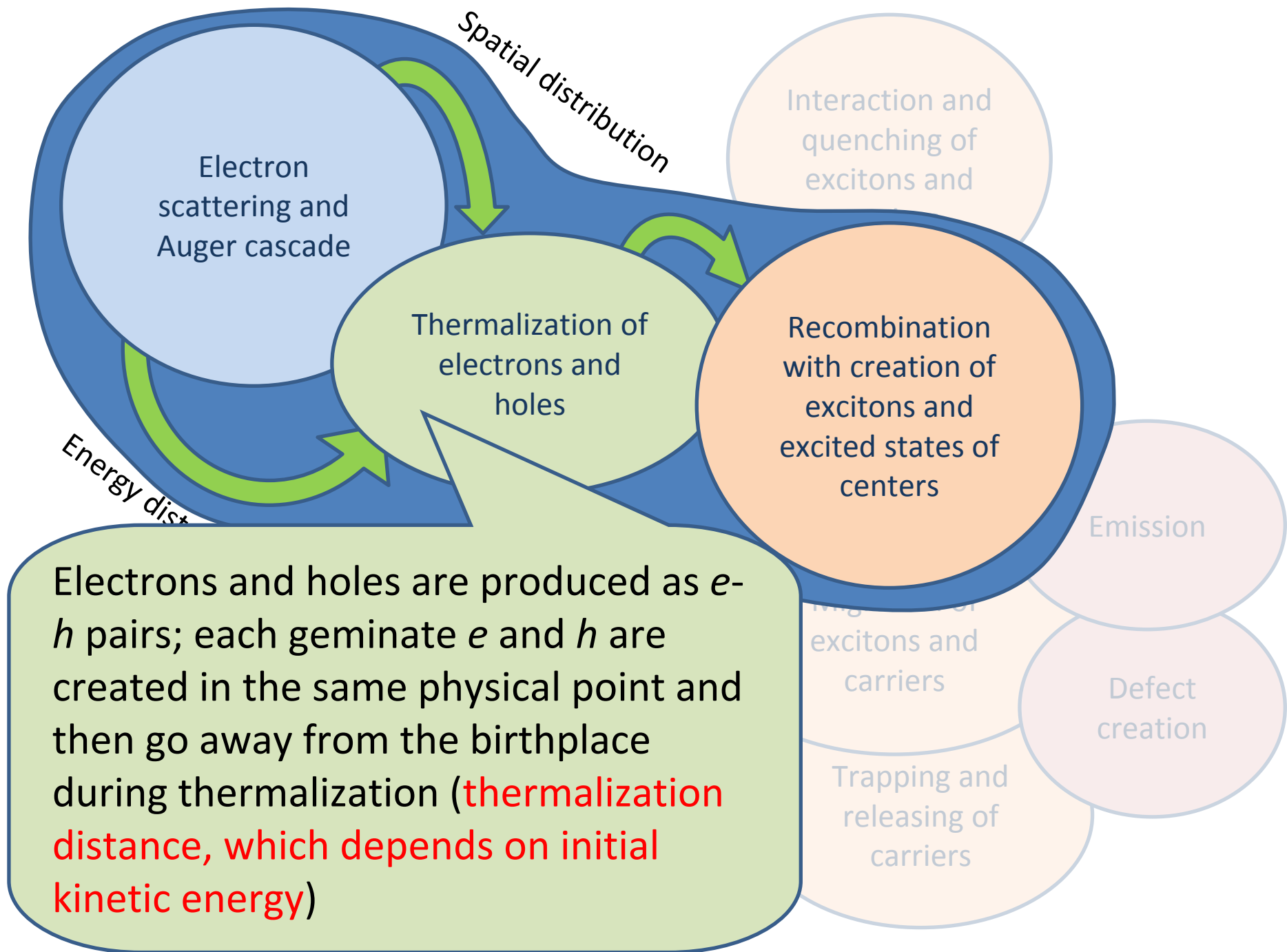
# Outline

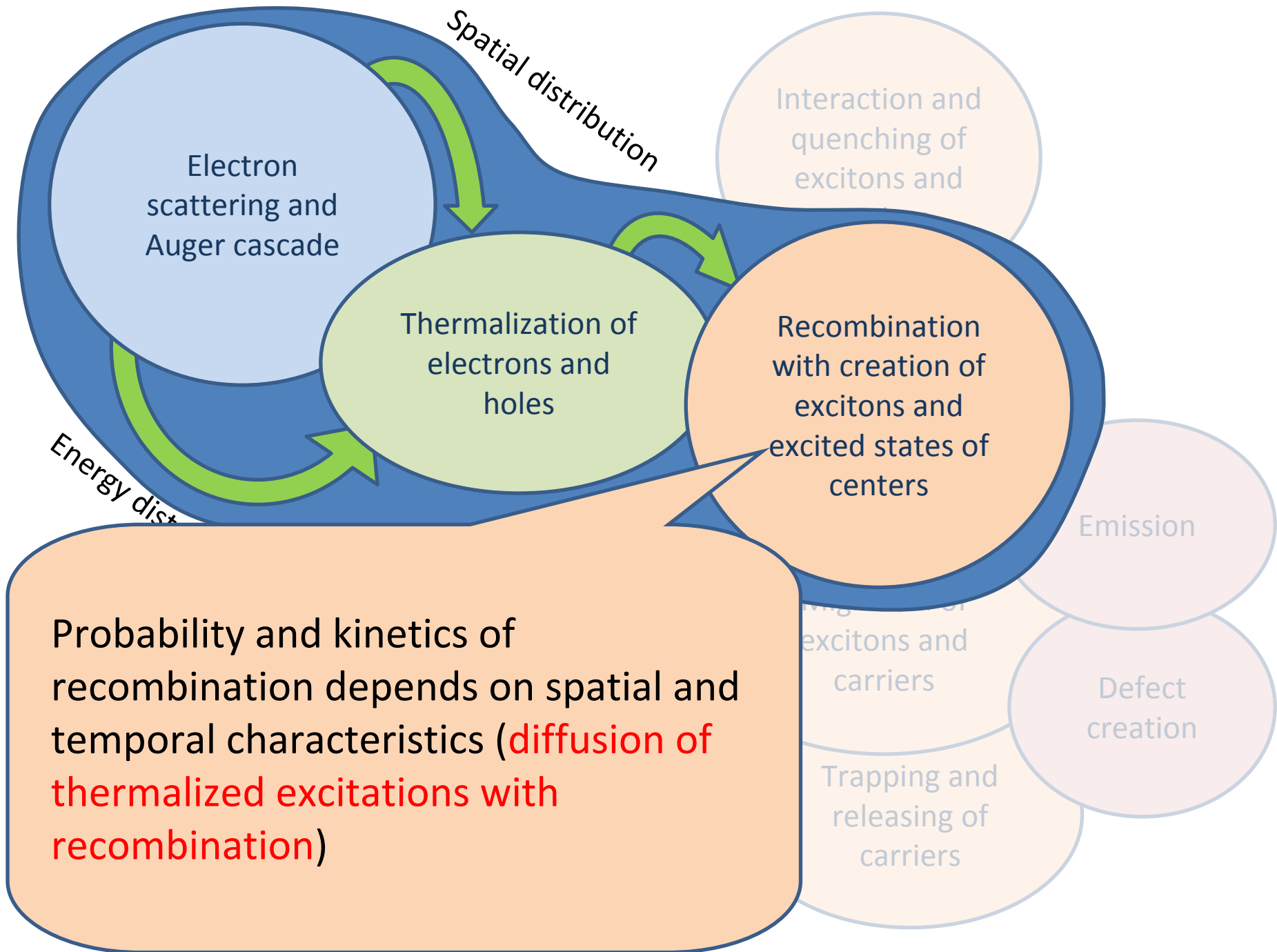
- Spatial scales for processes in scintillators
- Nanoparticles as scintillators
- **Cascade, thermalization and recombination**
- Different types of mobilities
- Thermalization length for different types of crystals
- Interconnection of cascade, thermalization and recombination stages in binary iodides
- Why cascade is so effective in CsI?
- Thermalization length and impurities
- Concluding remarks



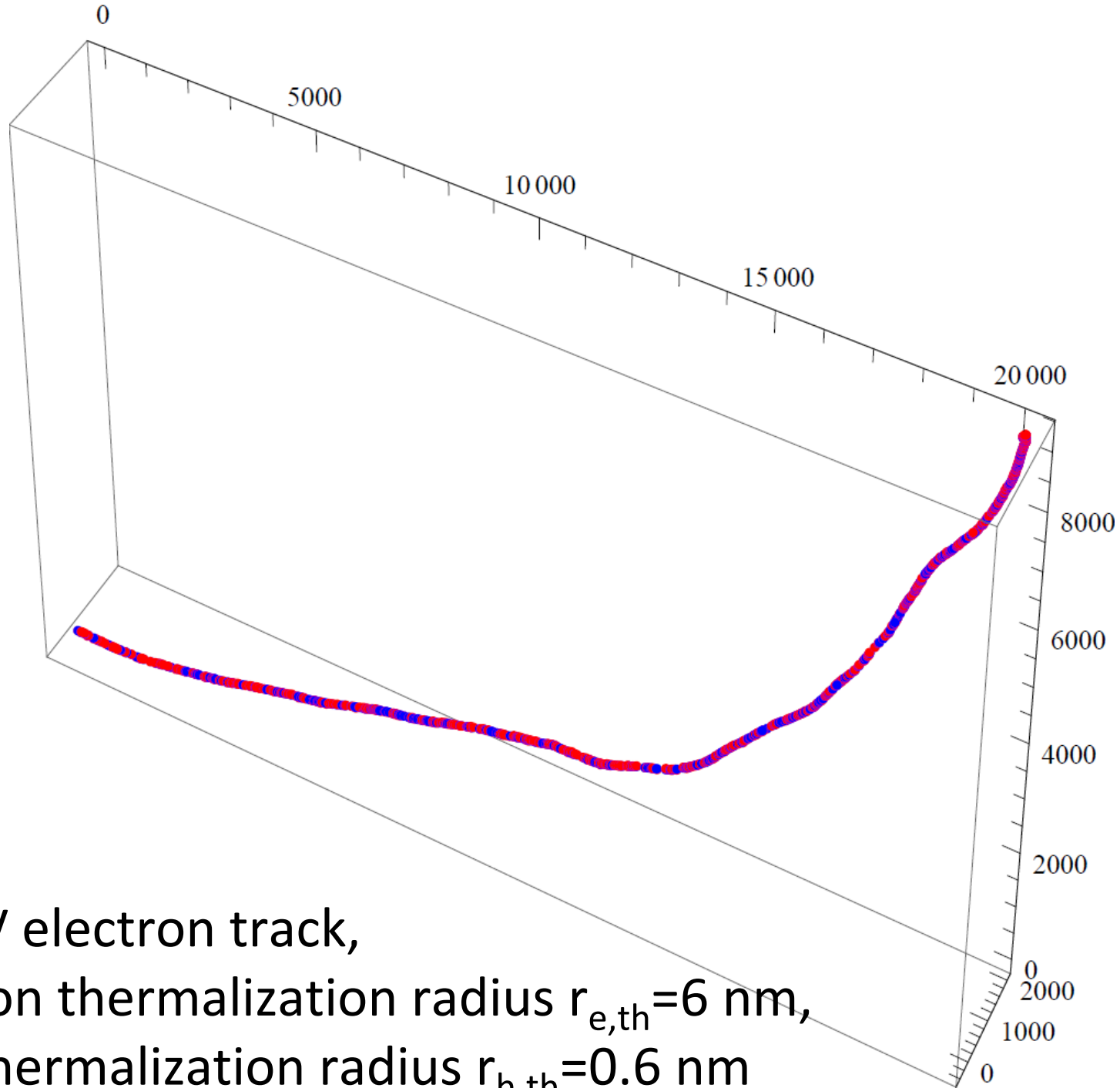




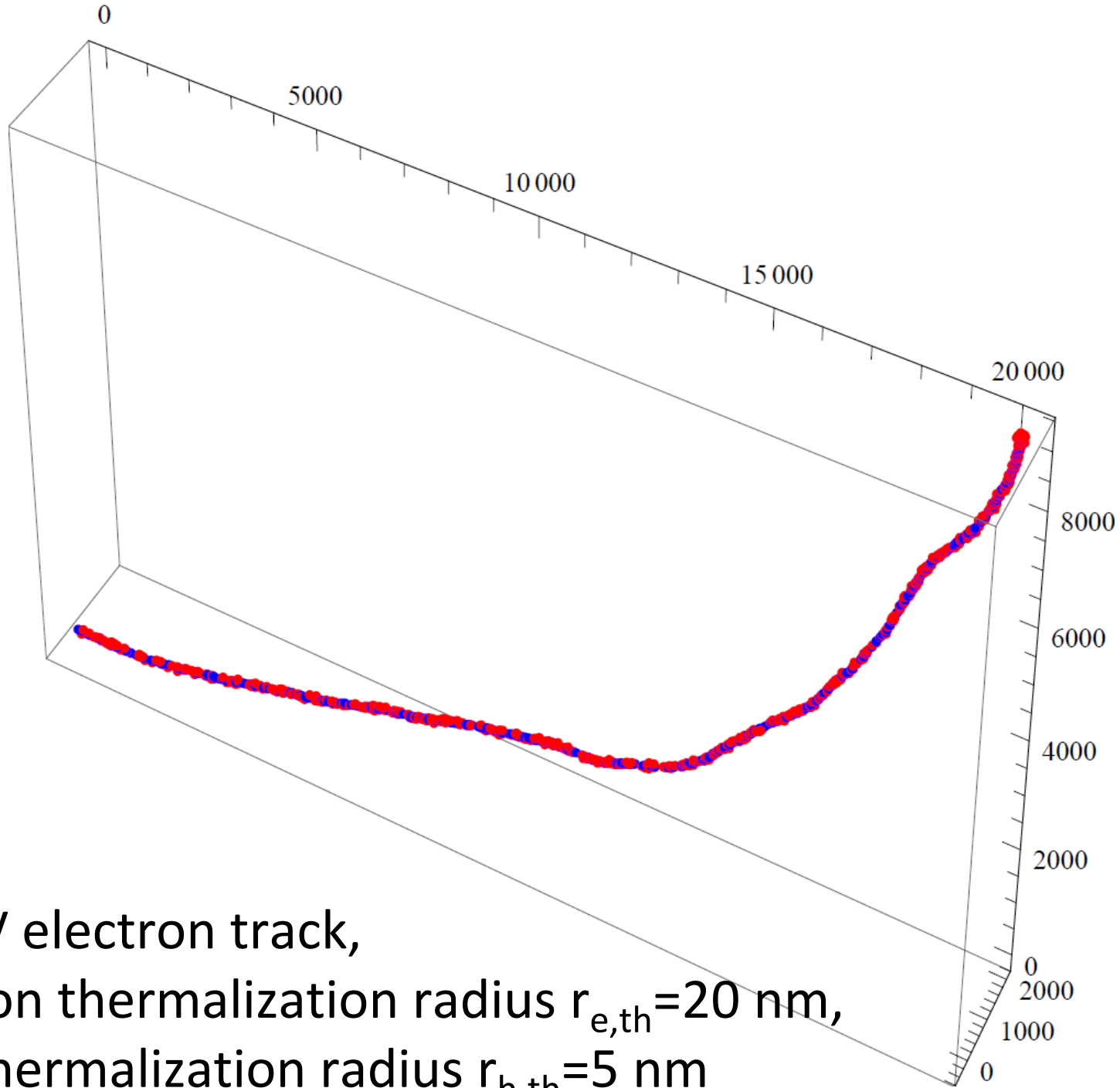




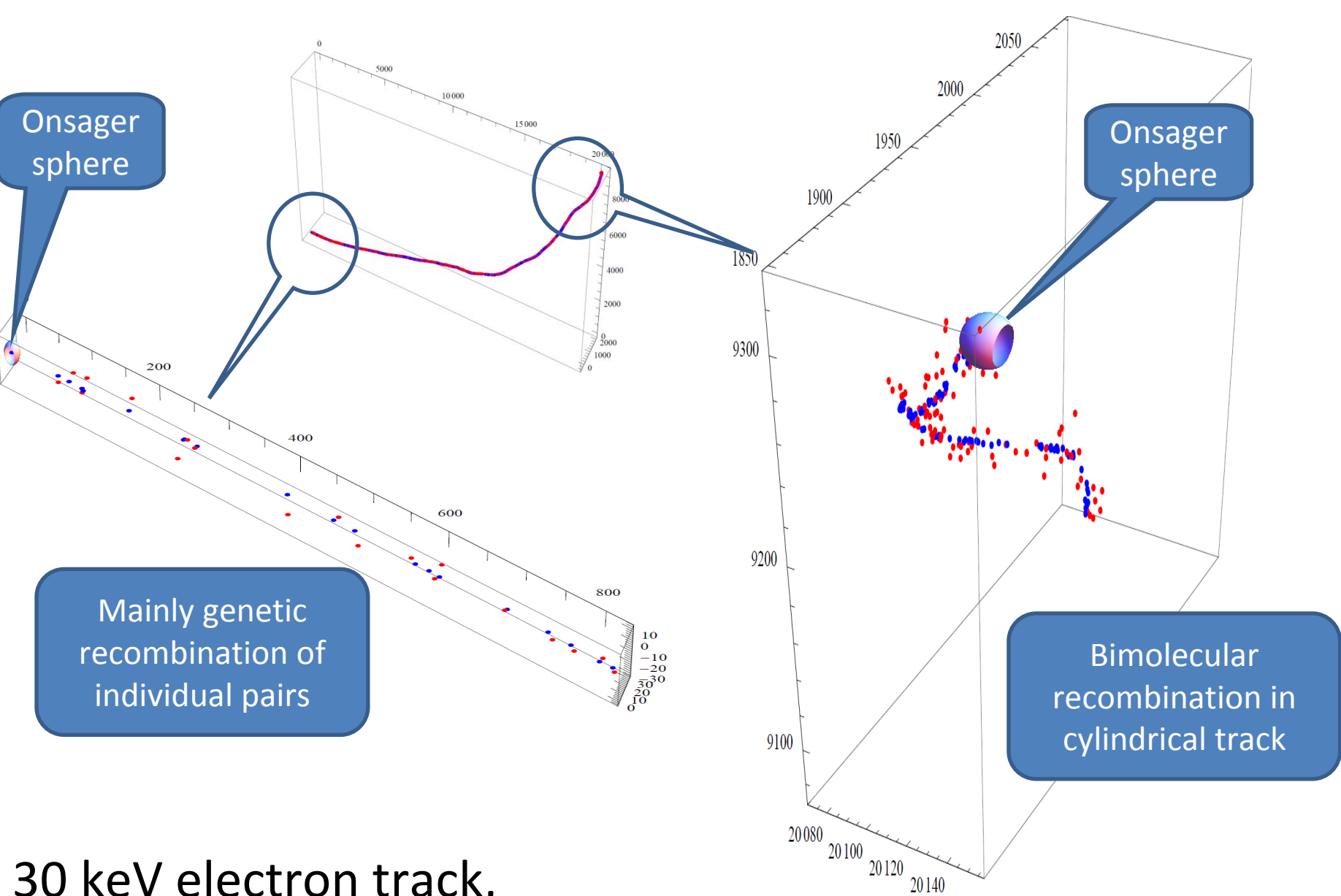
Example of structure of excited  
region after 30 keV electron  
passage



30 keV electron track,  
electron thermalization radius  $r_{e,th} = 6$  nm,  
hole thermalization radius  $r_{h,th} = 0.6$  nm

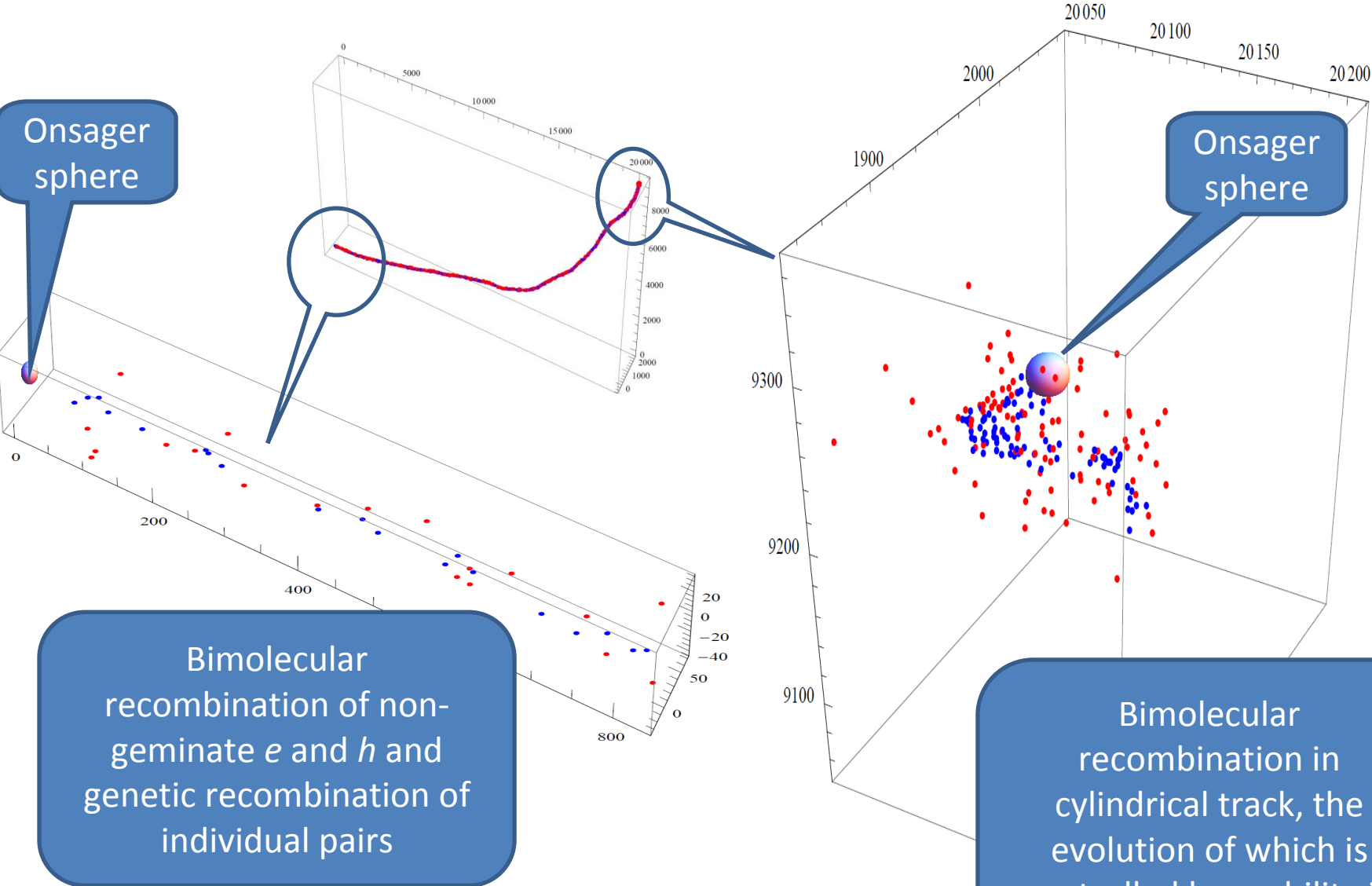


30 keV electron track,  
electron thermalization radius  $r_{e,th} = 20$  nm,  
hole thermalization radius  $r_{h,th} = 5$  nm



30 keV electron track,  
 $r_{e,th} = 6 \text{ nm}$ ,  
 $r_{h,th} = 0.6 \text{ nm}$  (red=e, blue=h)





30 keV electron track,  
 $r_{e,th} = 20$  nm,  
 $r_{h,th} = 5$  nm (red= $e$ , blue= $h$ )

# Outline

- Spatial scales for processes in scintillators
- Nanoparticles as scintillators
- Cascade, thermalization and recombination
- **Different types of mobilities**
- Thermalization length for different types of crystals
- Interconnection of cascade, thermalization and recombination stages in binary iodides
- Why cascade is so effective in CsI?
- Thermalization length and impurities
- Concluding remarks

# Non-proportionality and mobility

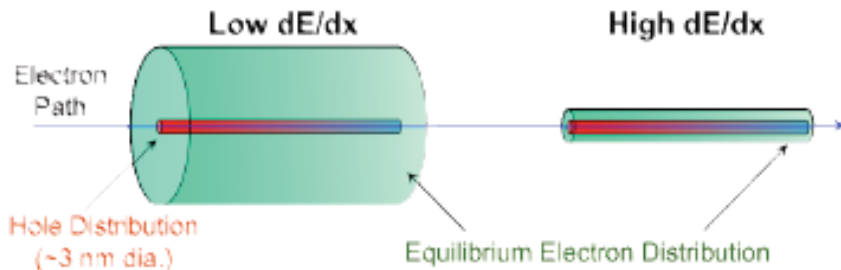


Figure 4. Difference between equilibrium diameters of the electrons (assuming immobile holes) for two different ionizations. Low density is on the left, high density is on the right.

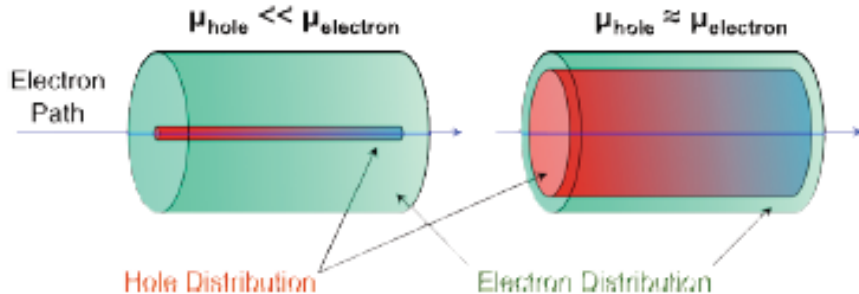


Figure 5. Relative sizes of electron and hole diameters as a function of relative hole mobility. The left side illustrates the distributions when the electron mobility is significantly higher than then hole mobility, while the right side illustrates the distributions when they have similar mobilities.

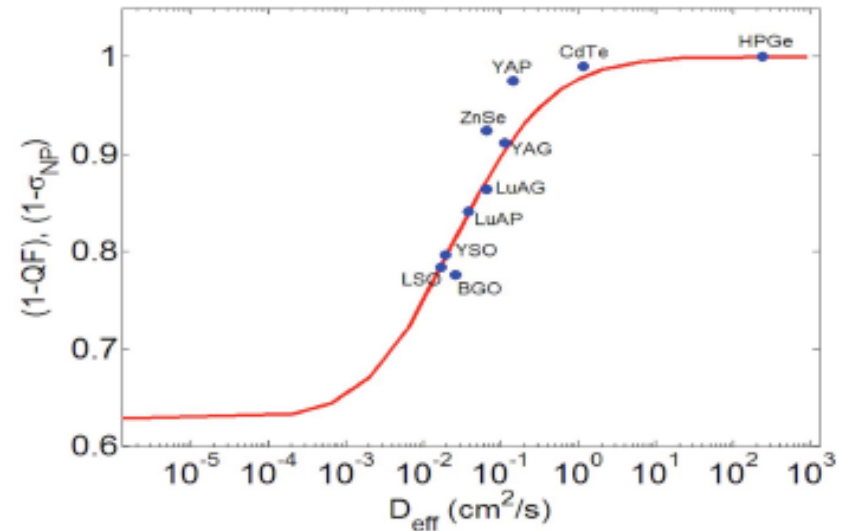


Figure 6. Measured relative light yield at low electron energy for a number of scintillators (solid points) and predicted luminosity (solid curve) as a function of diffusion coefficient. Reprinted with permission from [61]. See text for definitions.

W. W. Moses, G. A. Bizarri, R. T. Williams, S. A. Payne, A. N. Vasil'ev, J. Singh, Q. Li, J. Q. Grim, and W-S. Choong, *The Origins of Scintillator Non-Proportionality*, IEEE Transactions on Nuclear Science, vol. 59, issue 5, pp. 2038-2044 (2012)

# Spatial distribution of electrons, holes and excitons due to mobility in e-e passive energy domain

- Two types of carrier mobilities: **thermalization length (mobility of hot electrons and holes)** and **mobility of thermalized excitations (electrons, holes & excitons)**.
- High-energy part of ionization track – individual electron-hole pairs and small non-overlapping clusters of excitations. **Negative role of mobility**: the higher **the thermalization length** (in comparison with Onsager radius), the lower the recombination yield (HPGe – the limiting case of high mobility w/o any luminescence).
- Low-energy part of ionization track – overlapping clusters of excitations. Mean distance between interacting excitations increases with increase of the mobility of excitons. **Positive role of mobility**: the higher the mobility, the lower the quenching of excitation due to high EE density.
- “Ideal” scintillator: **Low hot mobility (high yield of excitons)** and **high thermalized mobility (low interaction)**.

# Outline

- Spatial scales for processes in scintillators
- Nanoparticles as scintillators
- Cascade, thermalization and recombination
- Different types of mobilities
- **Thermalization length for different types of crystals**
- Interconnection of cascade, thermalization and recombination stages in binary iodides
- Why cascade is so effective in CsI?
- Thermalization length and impurities
- Concluding remarks

# Coupled processes of thermalization and spatial diffusion

Four main functions which characterized spatial diffusion and thermalization:

(1) rate of electron-phonon scattering (inverse lifetime)  $\tau^{-1}(E_e^{kin})$

(2) mean free path  $\lambda(E_e^{kin}) = v(E_e^{kin})\tau(E_e^{kin})$

(3) spatial diffusion coefficient  $D^R(E_e^{kin}) = \frac{1}{3}v^2(E_e^{kin})\tau(E_e^{kin})$  and  
equation for Brownian motion

$$\frac{d \langle r^2 \rangle}{dt} = 6D^R(E_e^{kin})$$

(4) energy relaxation rate  $S(E_e^{kin}) = D^E(E_e^{kin})/k_B T$  and  
energy relaxation equation

$$\frac{dE_e^{kin}}{dt} = -S(E_e^{kin})$$

$$\frac{d \langle r^2 \rangle}{dE_e^{kin}} = -6 \frac{D^R(E_e^{kin})}{S(E_e^{kin})}$$

# Coupled processes of thermalization and spatial diffusion

Mean square of the thermalization distance  $\langle r^2 \rangle_{E_{e0} \rightarrow E_e^{kin}} = 6 \int_{E_e^{kin}}^{E_{e0}} \frac{D^R(E')}{S(E')} dE'$

Spatial distribution function  $f(r, l_e(E_{e0})) = \frac{3\sqrt{6} r^2}{\sqrt{\pi} l_e^3(E_{e0})} \exp\left(-\frac{3r^2}{2l_e^2(E_{e0})}\right)$

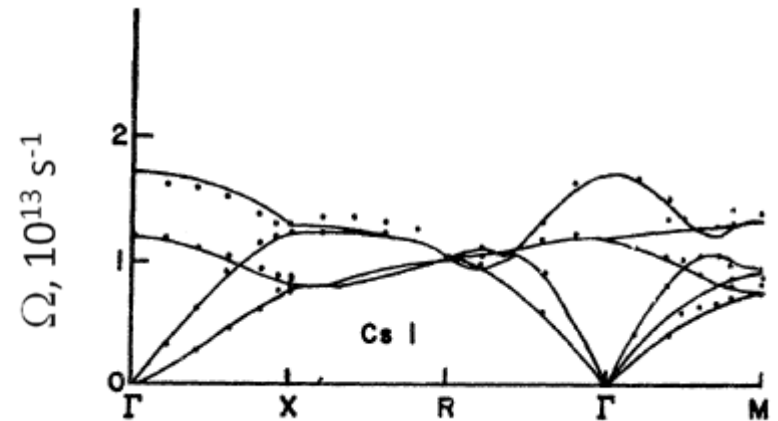
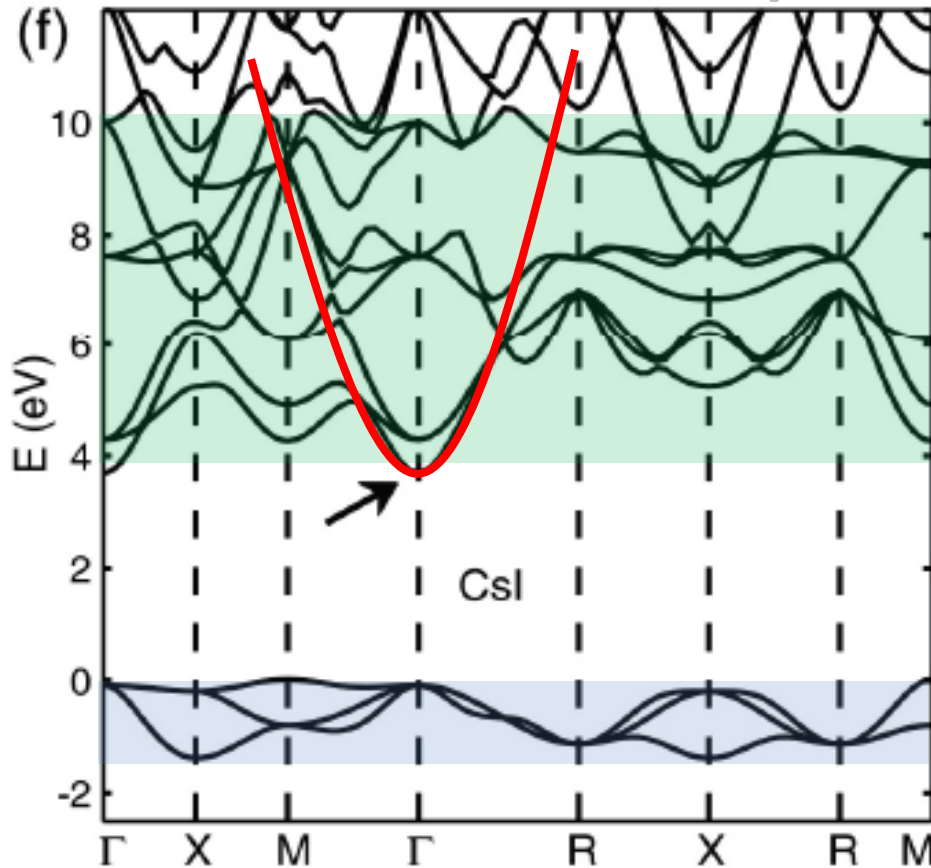
where thermalization length is  $l_e(E_{e0}) = \sqrt{\langle r^2 \rangle_{E_{e0} \rightarrow k_B T}}$

Thermalization length for one LO phonon branch

$$l_{e,LO}^2(E_{e0}) = \frac{8}{3} a_B^2 \left( \frac{\tilde{\epsilon}}{m_e^*/m_0} \right)^2 \tanh\left(\frac{\hbar\Omega_{LO}}{2k_B T}\right) \int_{\hbar\Omega_{LO}}^{E_{e0}} \left( \frac{E'}{\hbar\Omega_{LO}} \right)^2 \frac{1}{\ln(4E'/\hbar\Omega_{LO})} \frac{dE'}{\hbar\Omega_{LO}}$$

$$= \frac{1}{24} a_B^2 \left( \frac{\tilde{\epsilon}}{m_e^*/m_0} \right)^2 \tanh\left(\frac{\hbar\Omega_{LO}}{2k_B T}\right) \text{Ei}\left(3 \ln\left(\frac{4E_{e0}}{\hbar\Omega_{LO}}\right)\right),$$

# CsI band structure and phonon dispersion



J.F. Vetelino, K. V. Namjoshi and S. S. Mitra,  
Phys. Rev. B 7, 4001–4004 (1973)

Band structure calculations

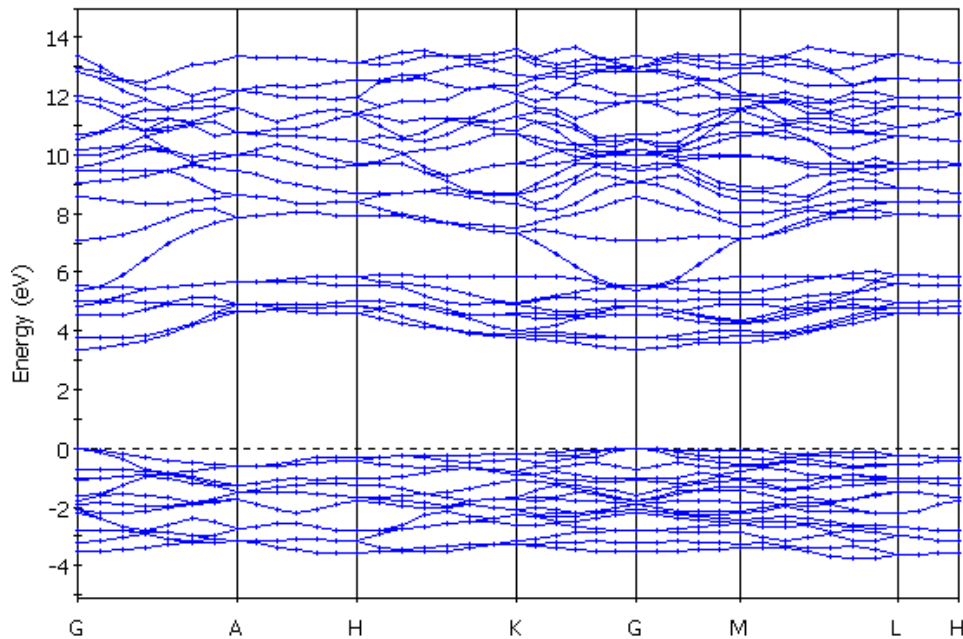
from W. Setyawan, R. M. Gaume et al. *IEEE TNS*, 2009



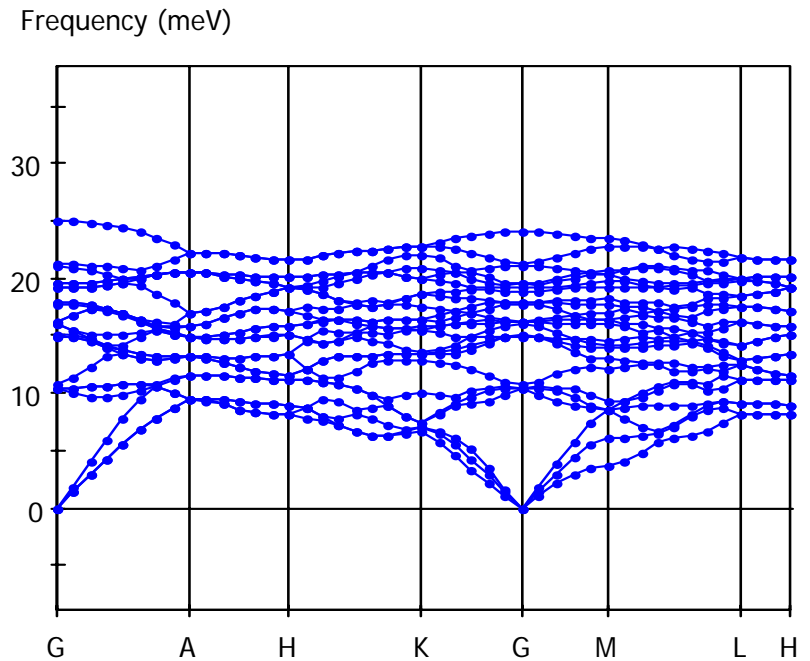
# LaBr<sub>3</sub> band structure (w/o La4f) and phonon dispersion

I.Iskandarova, private communication

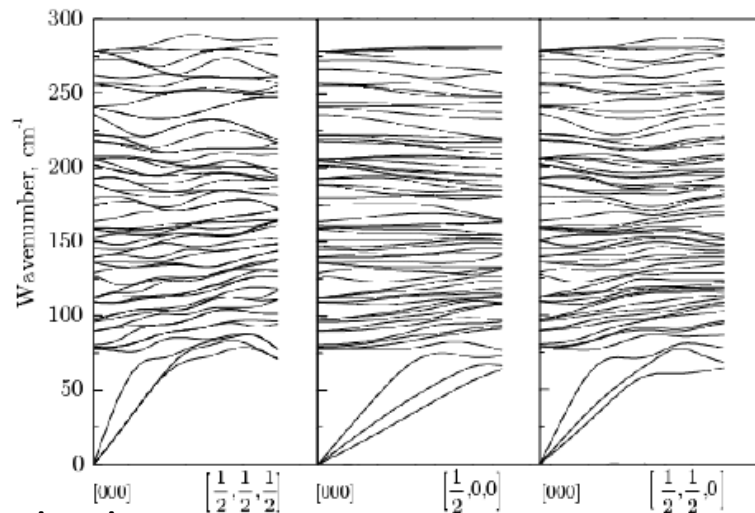
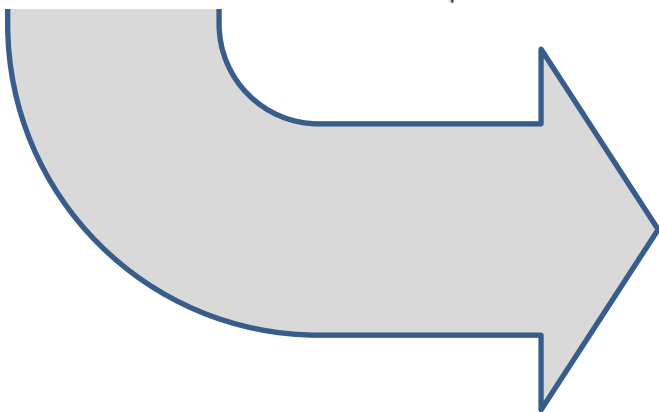
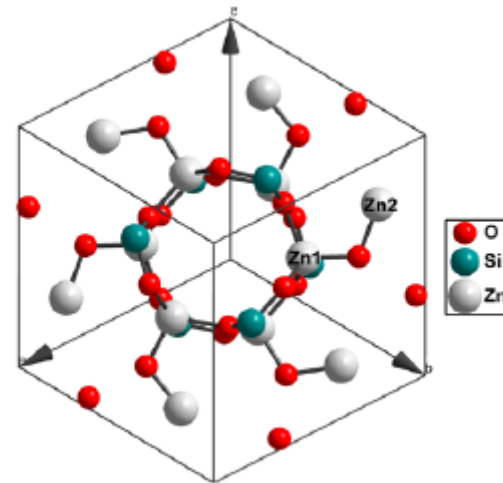
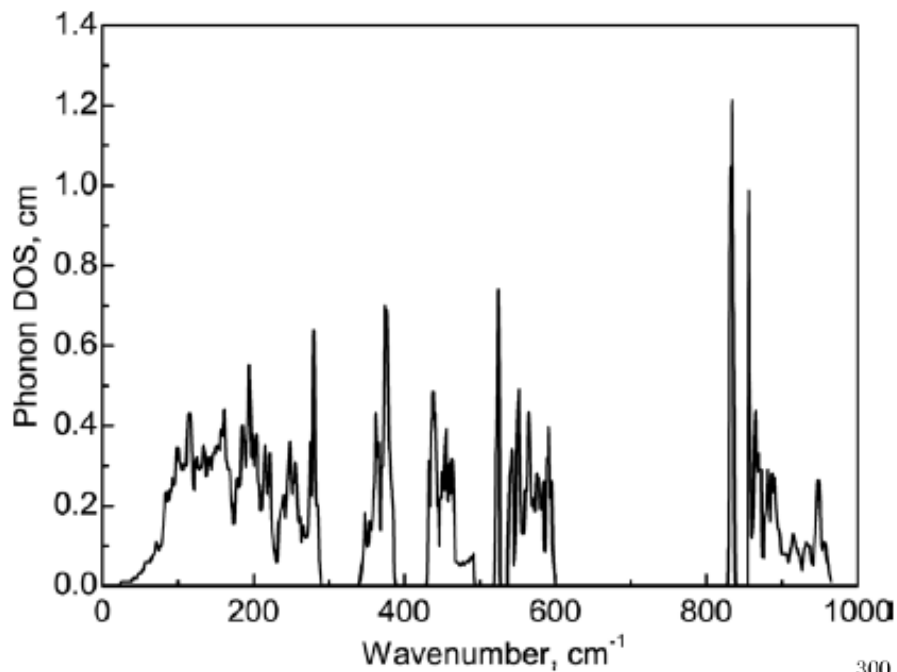
CASTEP Phonon Dispersion



Band structure for LaBr<sub>3</sub> (without La f states). Energy scale is shifted to the top of the valence band.



# Zn<sub>2</sub>SiO<sub>4</sub> (42 atoms per unit cell)

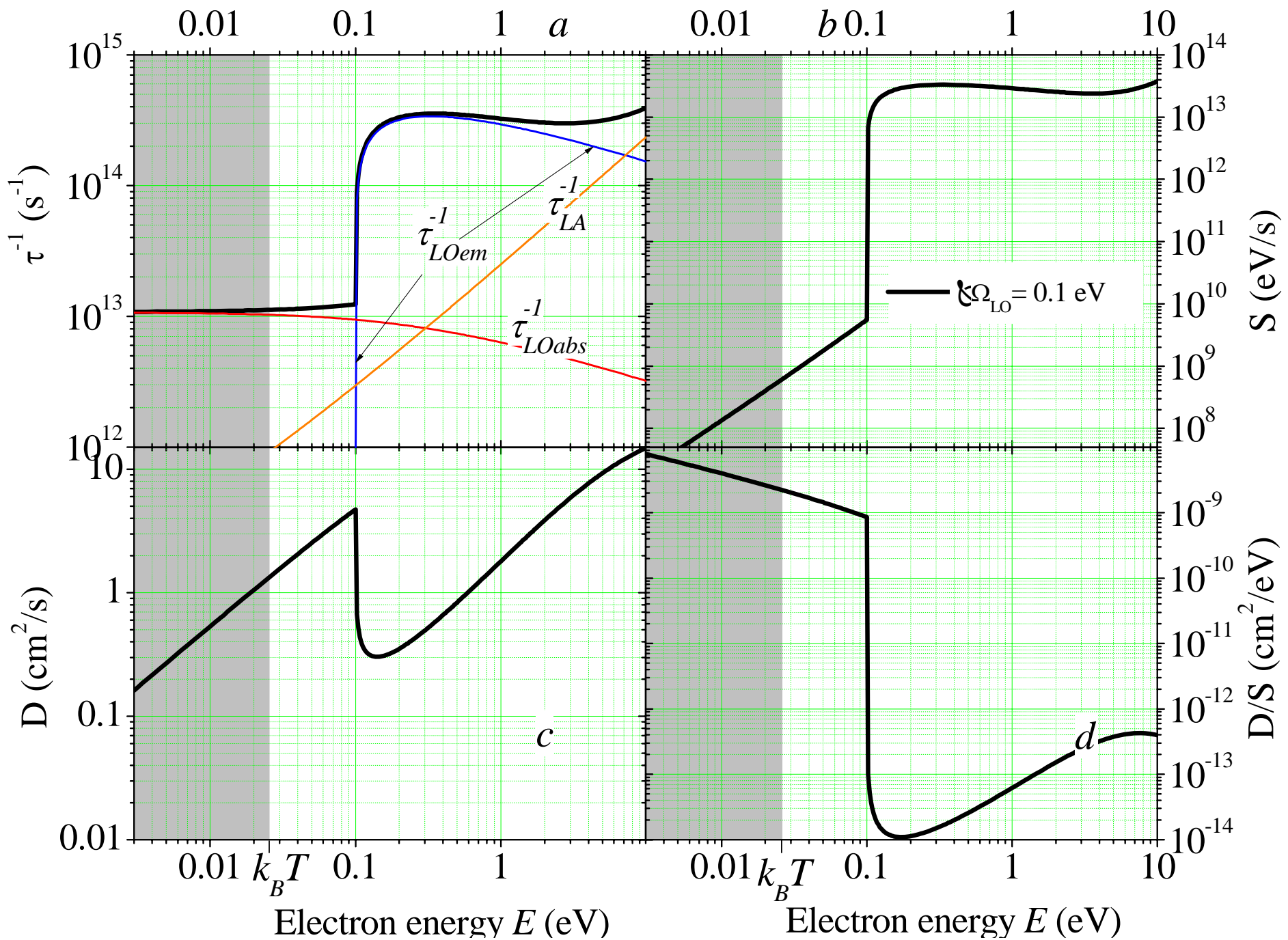


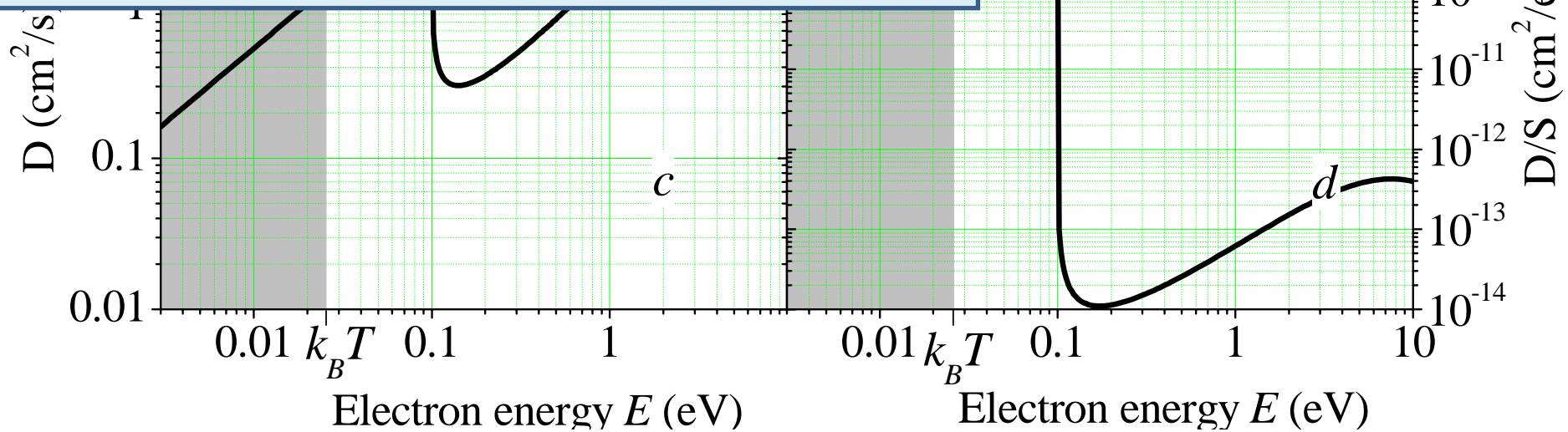
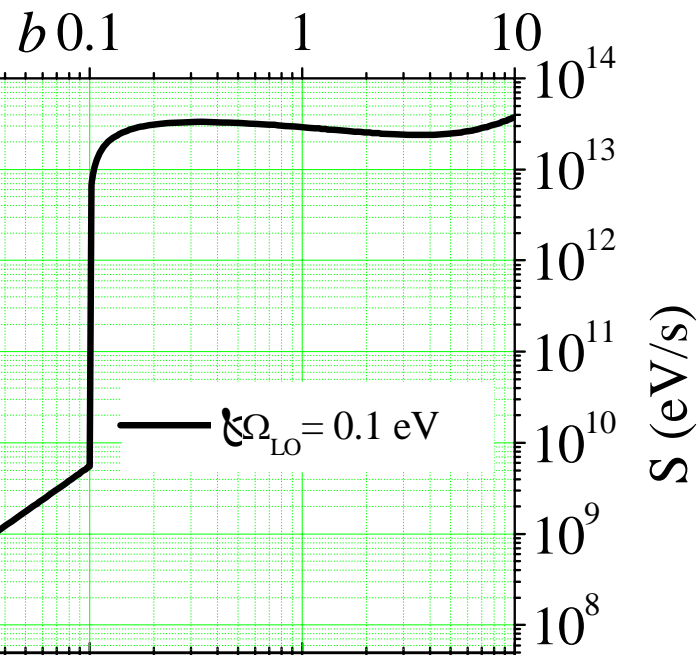
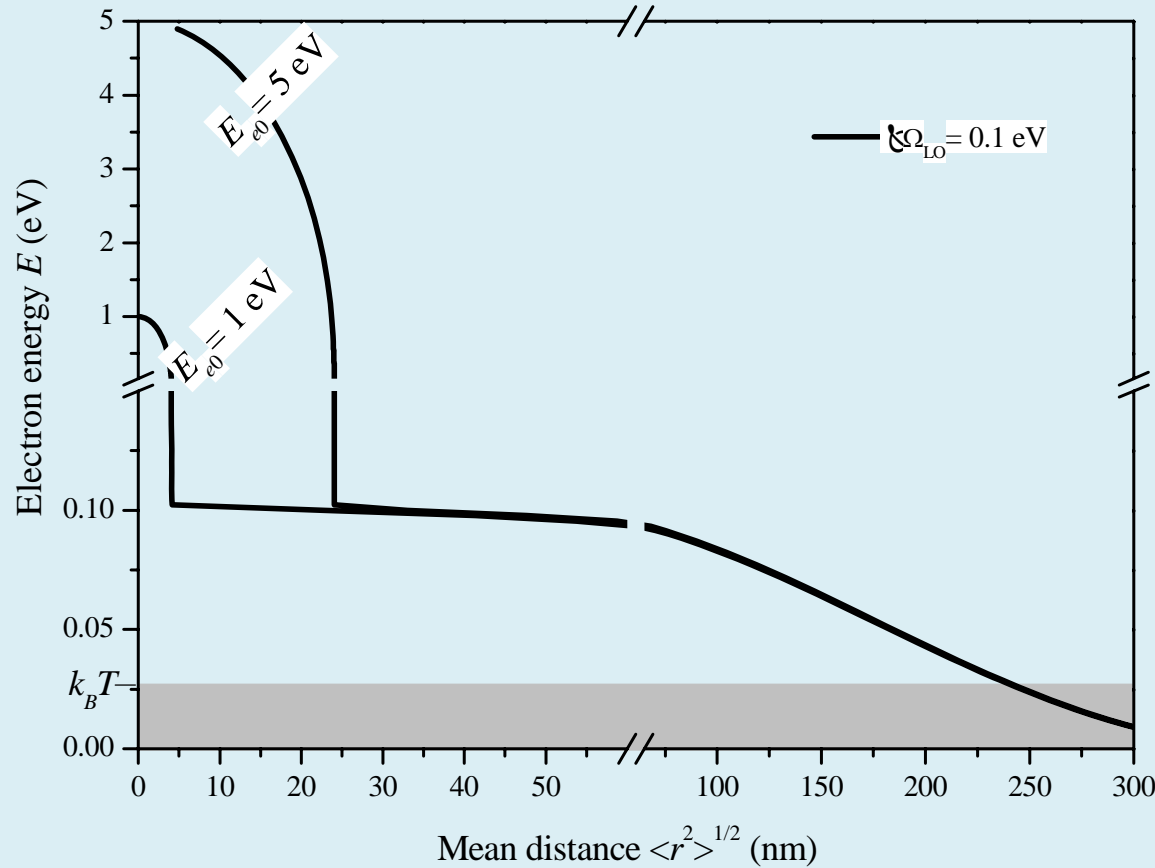
# Different cases to discuss

R.Kirkin, V.V. Mikhailin, and A.N. Vasil'ev, *Recombination of correlated electron-hole pairs with account of hot capture with emission of optical phonons*, IEEE Transactions on Nuclear Science, vol. 59, issue 5, pp. 2057-2064 (2012)

- Simple oxide or fluoride (one LO branch)

$$\hbar\Omega_{LO} = 0.1 \text{ eV} > k_B T = 300 \text{ K} = 0.026 \text{ eV}$$





# Different cases to discuss

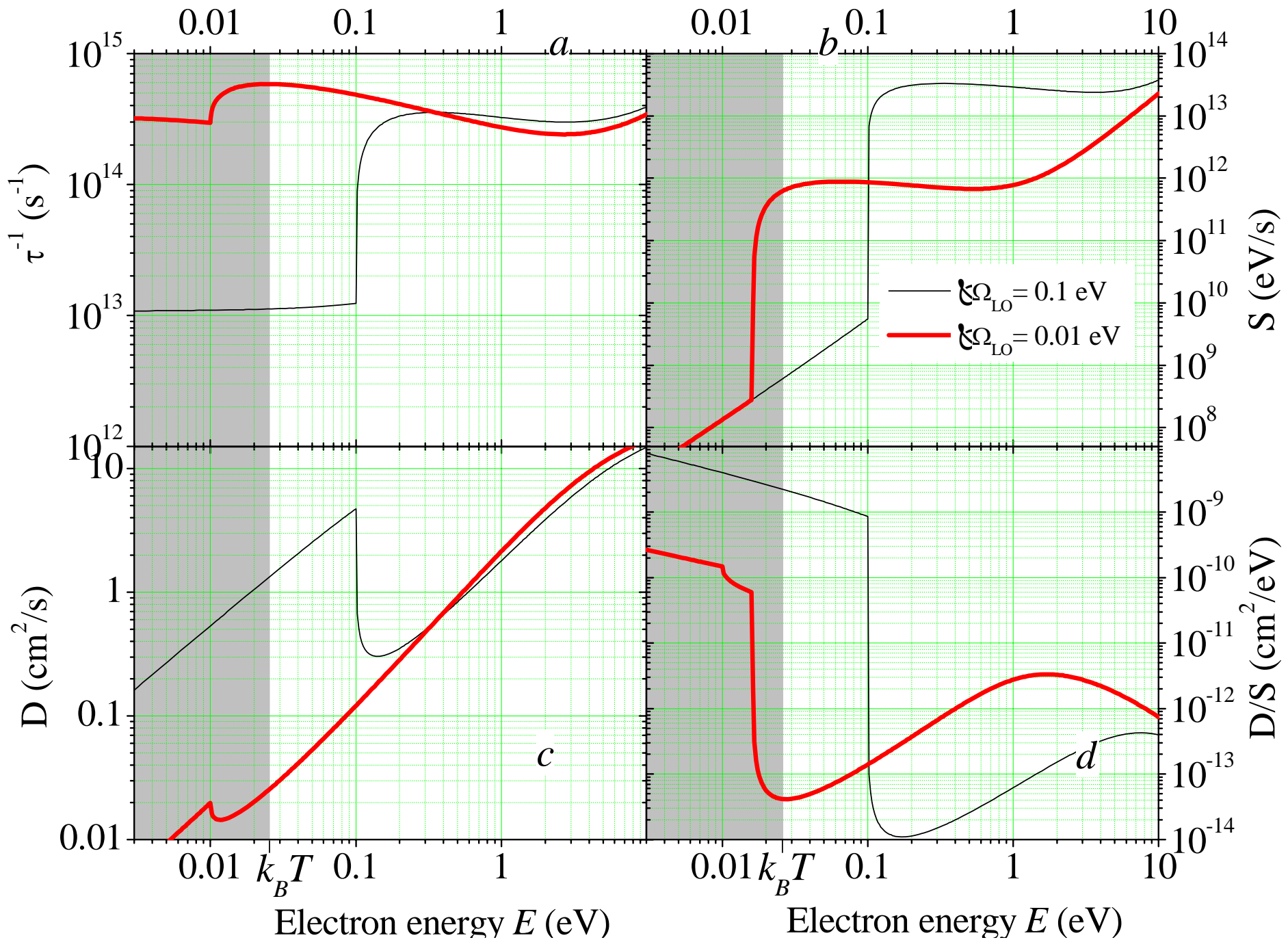
R.Kirkin, V.V. Mikhailin, and A.N. Vasil'ev, *Recombination of correlated electron-hole pairs with account of hot capture with emission of optical phonons*, IEEE Transactions on Nuclear Science, vol. 59, issue 5, pp. 2057-2064 (2012)

- Simple oxide or fluoride (one LO branch)

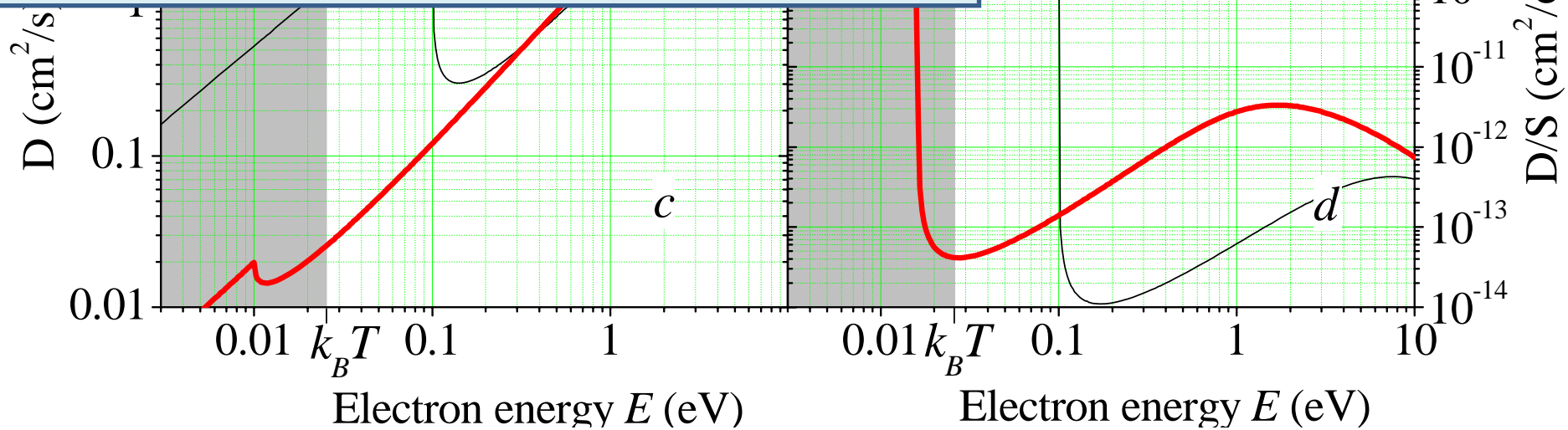
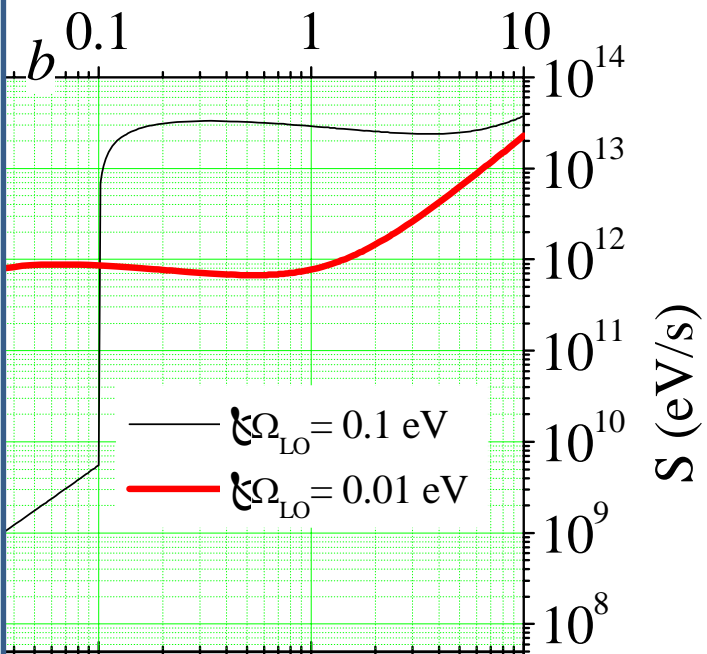
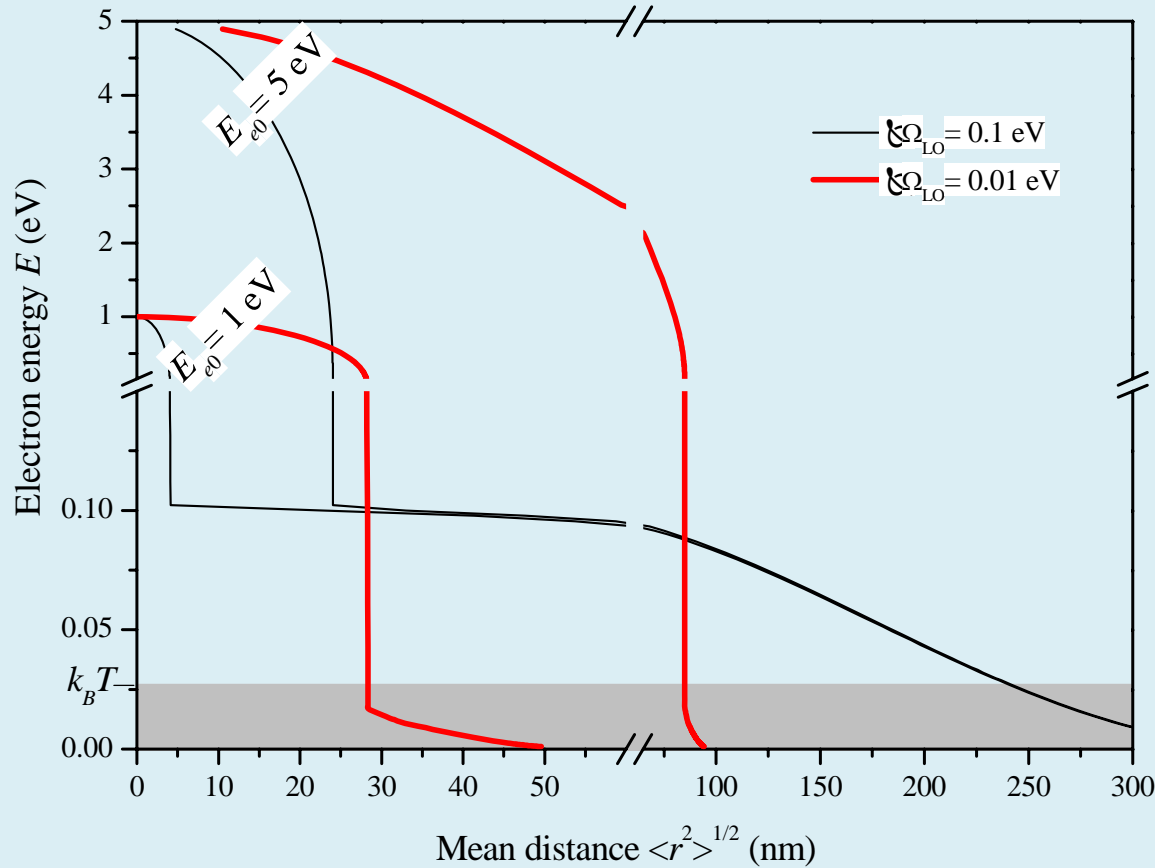
$$\hbar\Omega_{LO} = 0.1 \text{ eV} > k_B T = 300\text{K} = 0.026 \text{ eV}$$

- Simple iodide (e.g. CsI, one LO branch)

$$\hbar\Omega_{LO} = 0.01 \text{ eV} < k_B T$$









# Different cases to discuss

R.Kirkin, V.V. Mikhailin, and A.N. Vasil'ev, *Recombination of correlated electron-hole pairs with account of hot capture with emission of optical phonons*, IEEE Transactions on Nuclear Science, vol. 59, issue 5, pp. 2057-2064 (2012)

- Simple oxide or fluoride (one LO branch)

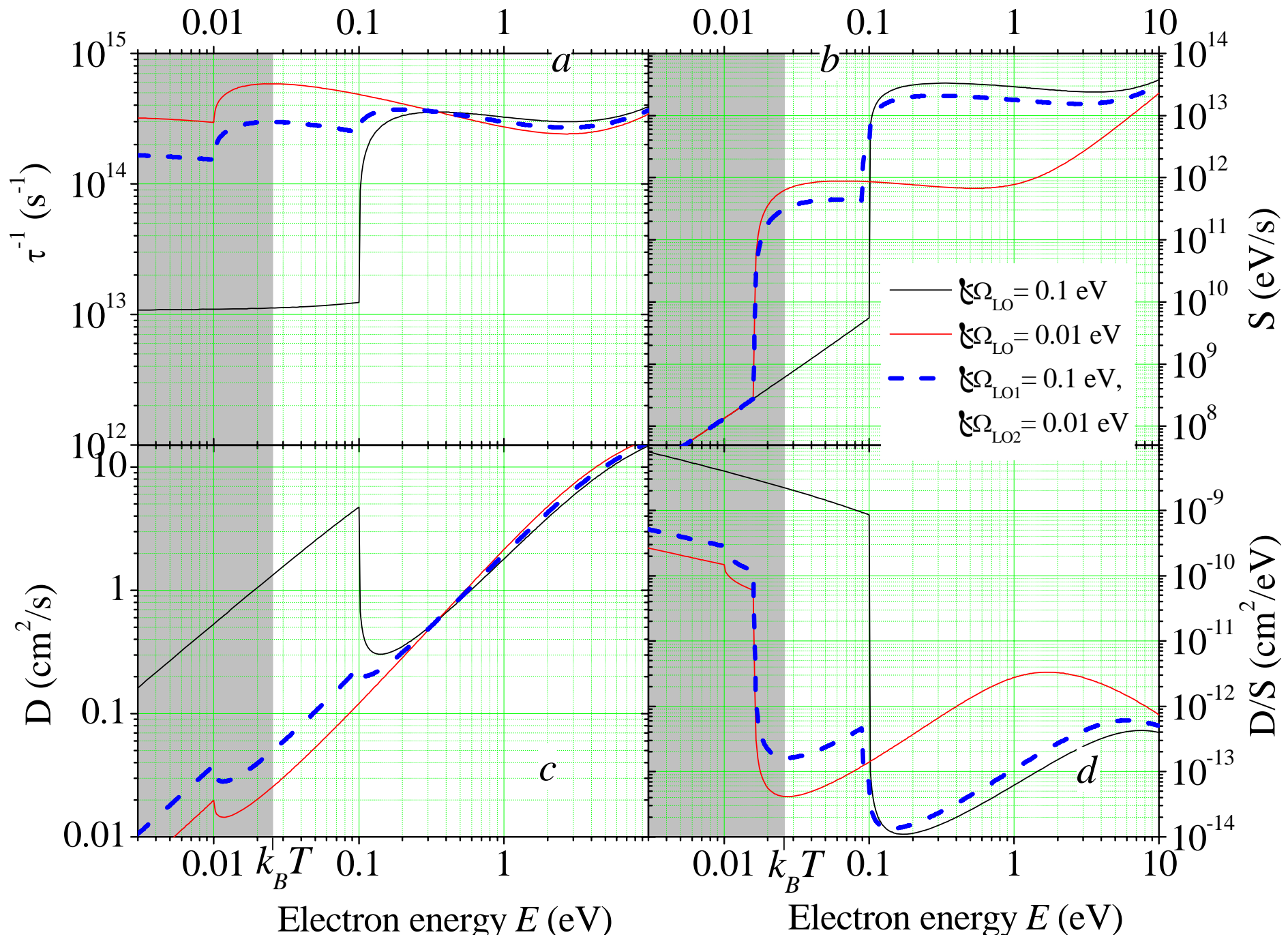
$$\hbar\Omega_{LO} = 0.1 \text{ eV} > k_B T = 300 \text{ K} = 0.026 \text{ eV}$$

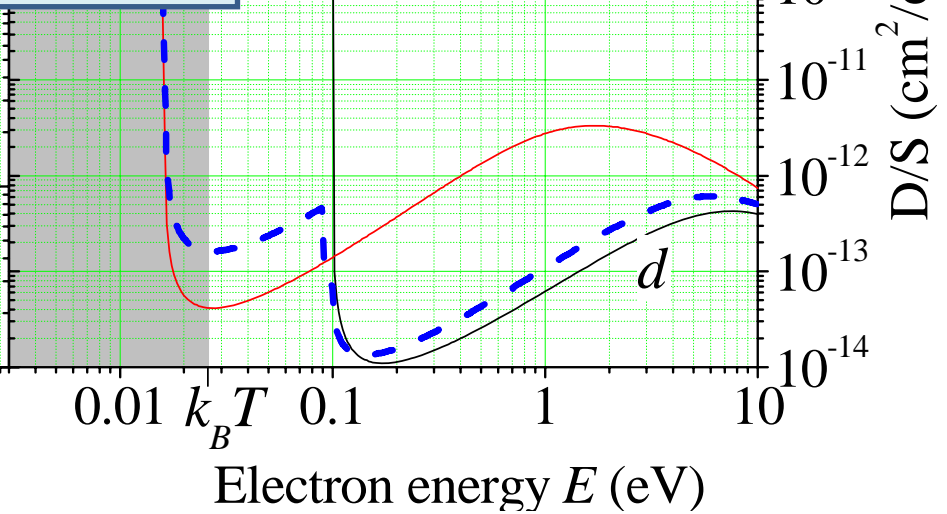
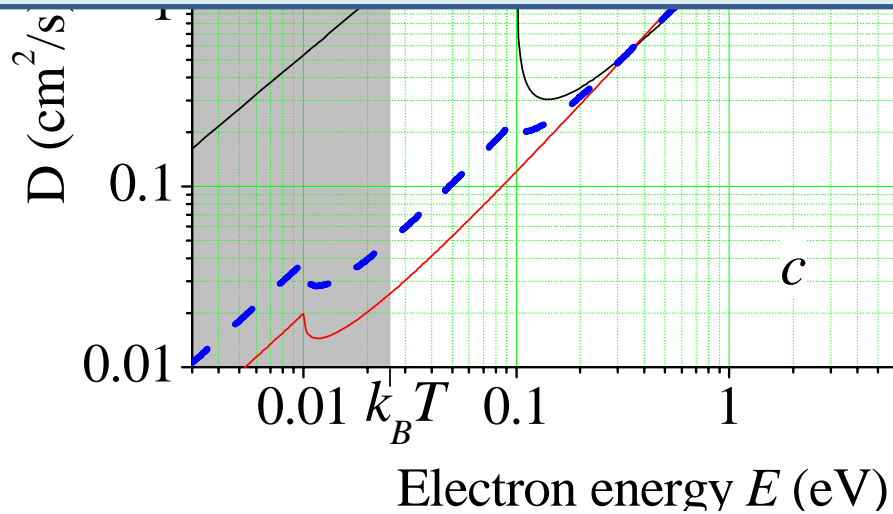
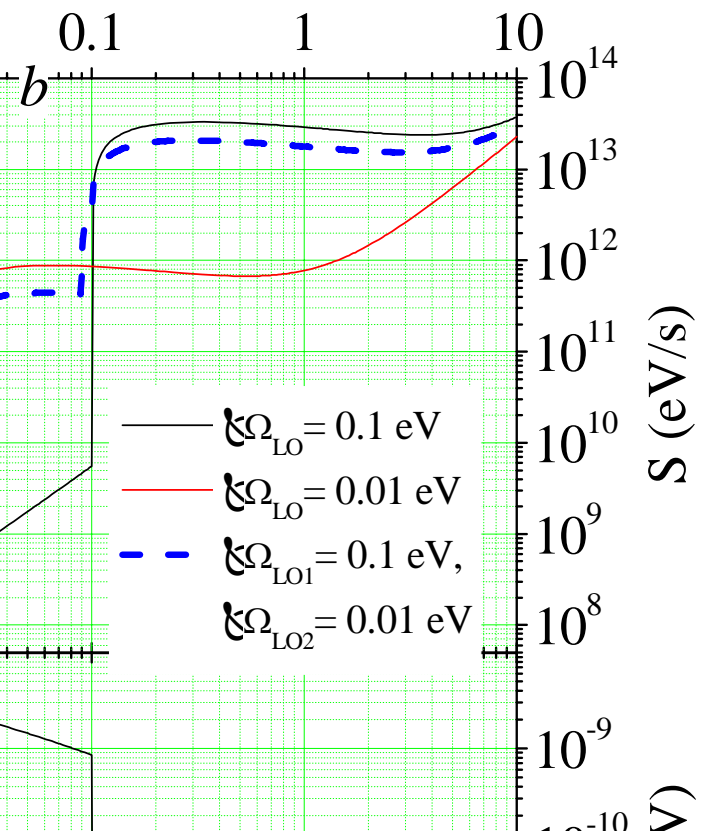
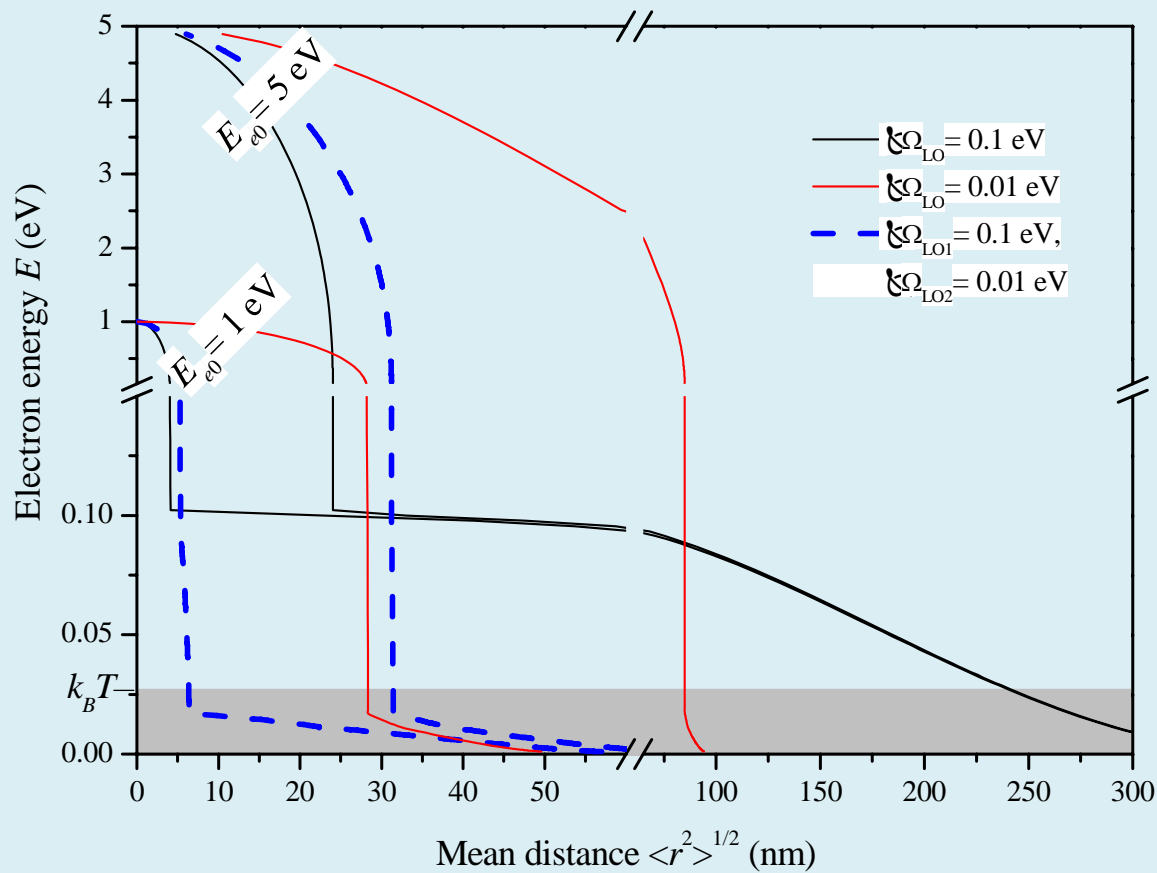
- Simple iodide (e.g. CsI, one LO branch)

$$\hbar\Omega_{LO} = 0.01 \text{ eV} < k_B T$$

- 2 LO branches with significantly different energies

$$\hbar\Omega_{LO1} = 0.1 \text{ eV}, \hbar\Omega_{LO2} = 0.01 \text{ eV}$$





# Different cases to discuss

R.Kirkin, V.V. Mikhailin, and A.N. Vasil'ev, *Recombination of correlated electron-hole pairs with account of hot capture with emission of optical phonons*, IEEE Transactions on Nuclear Science, vol. 59, issue 5, pp. 2057-2064 (2012)

- Simple oxide or fluoride (one LO branch)

$$\hbar\Omega_{LO} = 0.1 \text{ eV} > k_B T = 300\text{K} = 0.026 \text{ eV}$$

- Simple iodide (e.g. CsI, one LO branch)

$$\hbar\Omega_{LO} = 0.01 \text{ eV} < k_B T$$

- 2 LO branches with significantly different energies

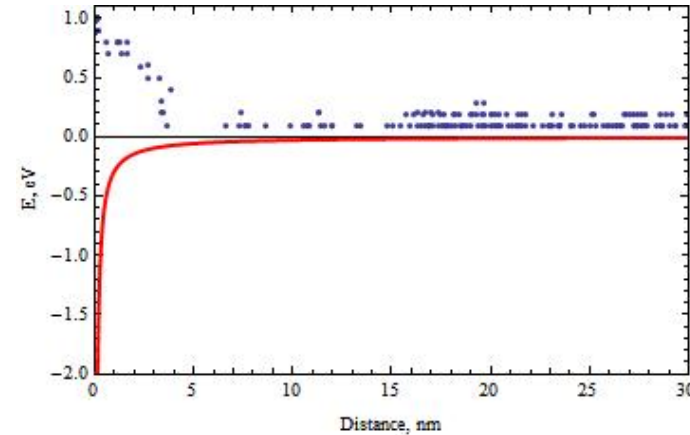
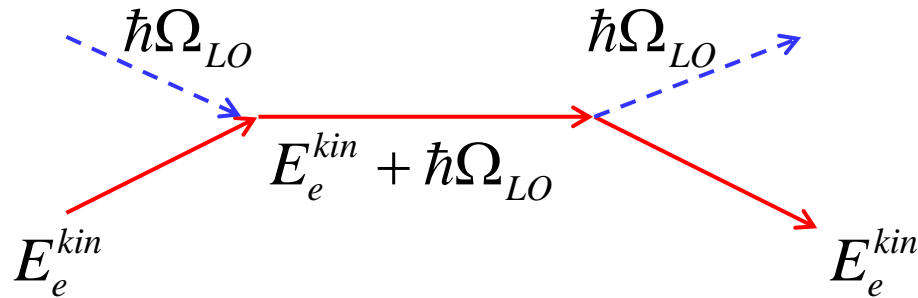
$$\hbar\Omega_{LO1} = 0.1 \text{ eV}, \hbar\Omega_{LO2} = 0.01 \text{ eV}$$

- 2 LO branches with close energies

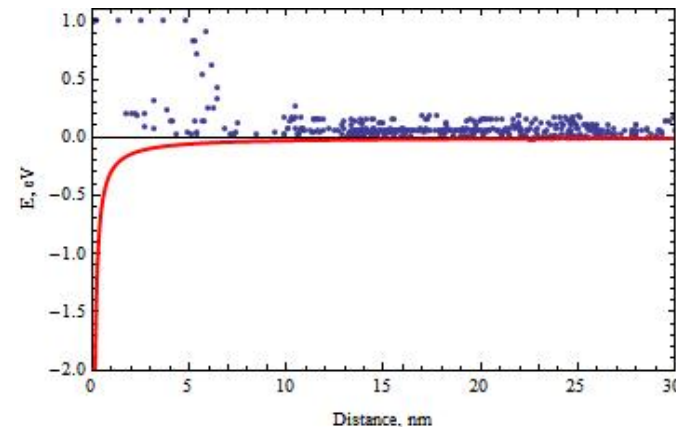
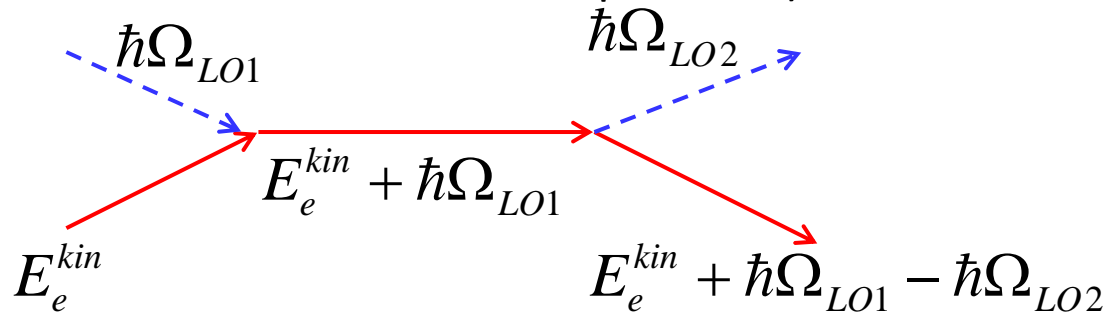
$$\hbar\Omega_{LO1} = 0.1 \text{ eV}, \hbar\Omega_{LO2} = 0.08 \text{ eV}$$

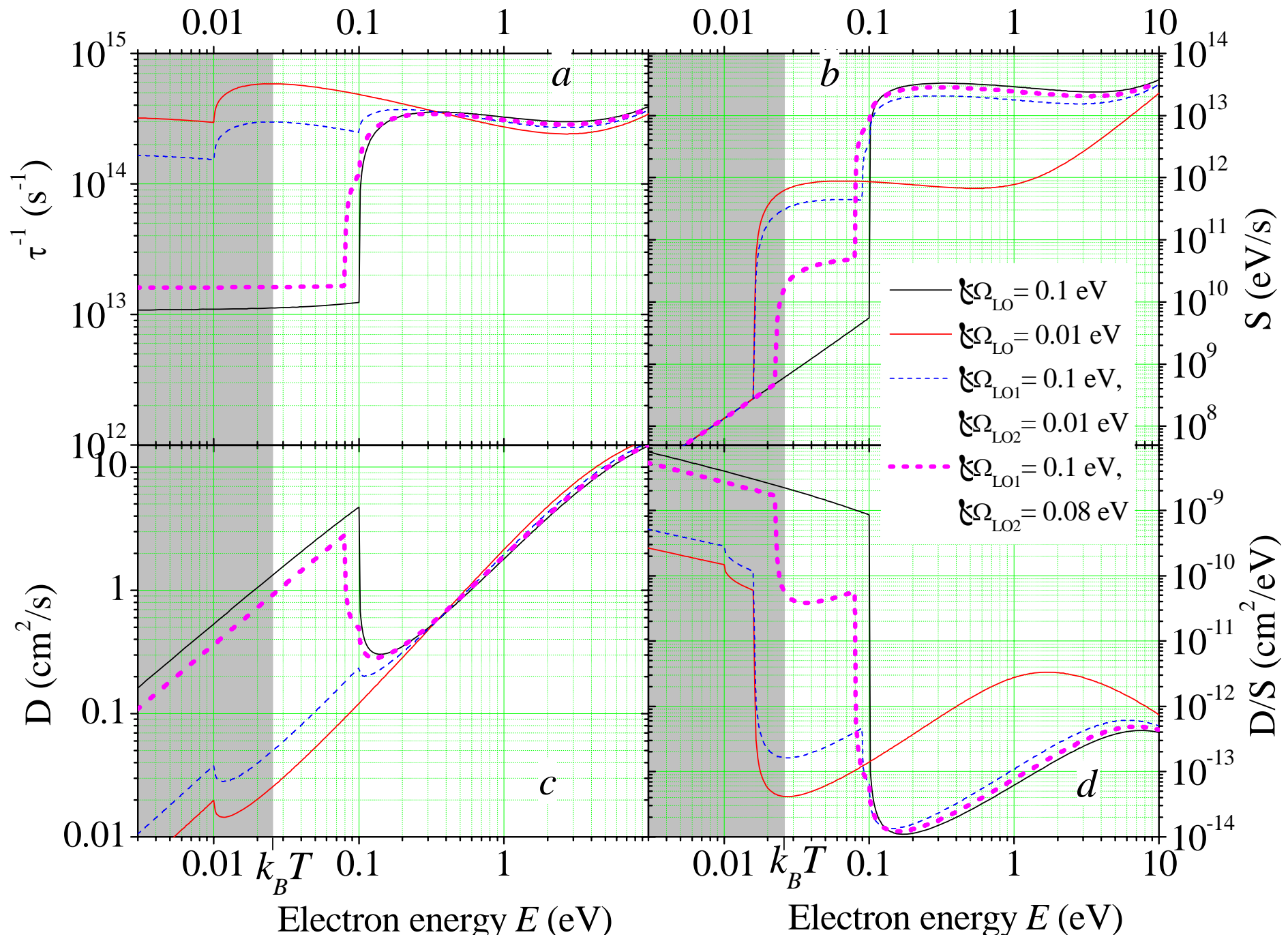
# Interaction with LO phonons in LO-passive region

- One LO branch (2 atoms/unit cell) – Spatial diffusion is due to LO phonons, and energy relaxation is due to LA phonons)

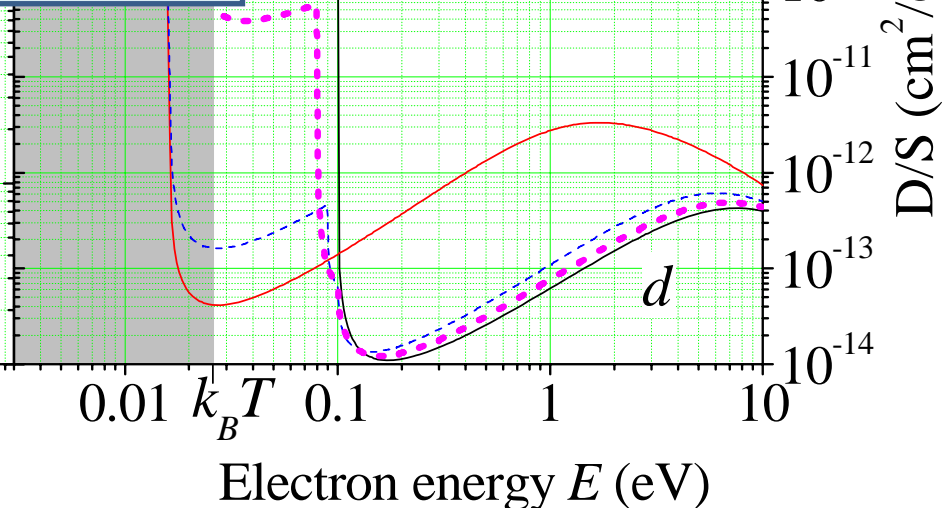
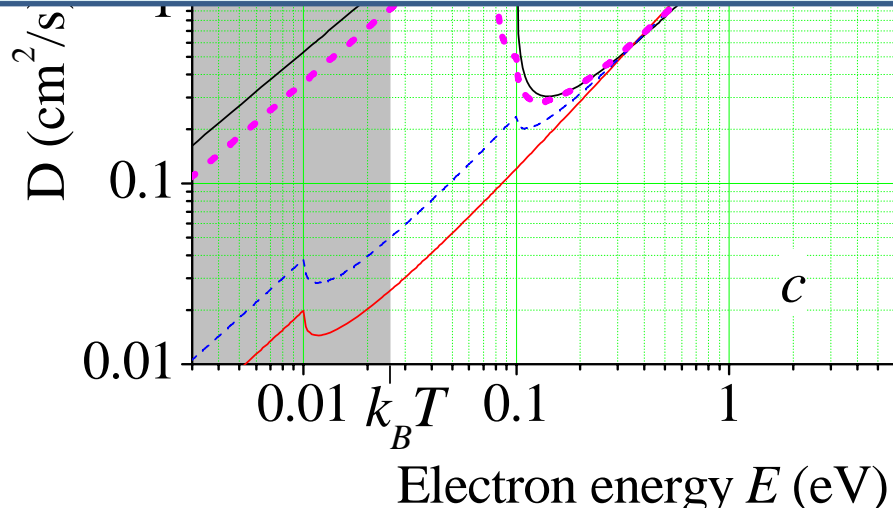
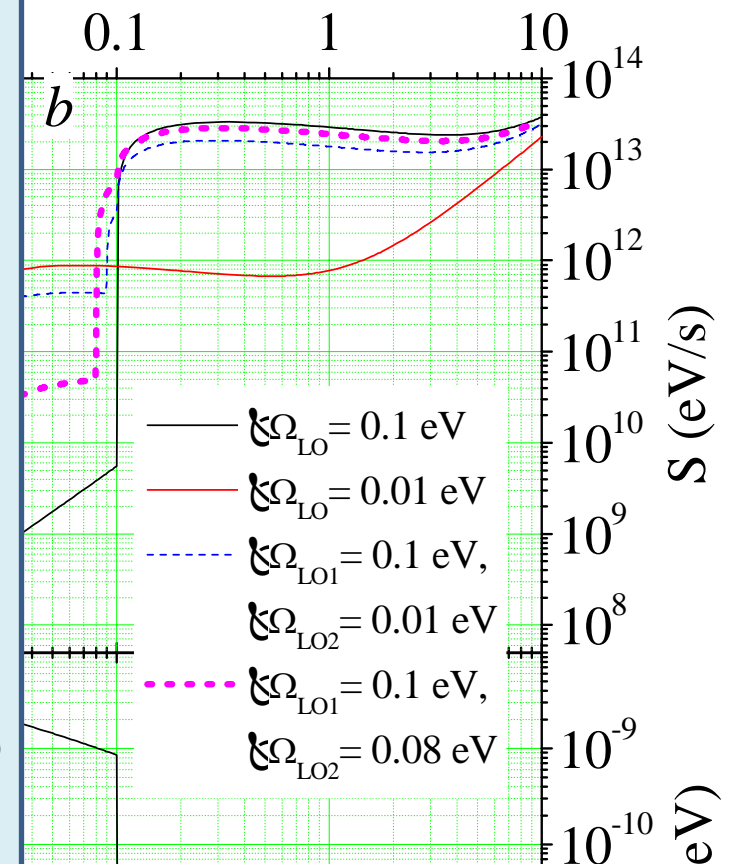
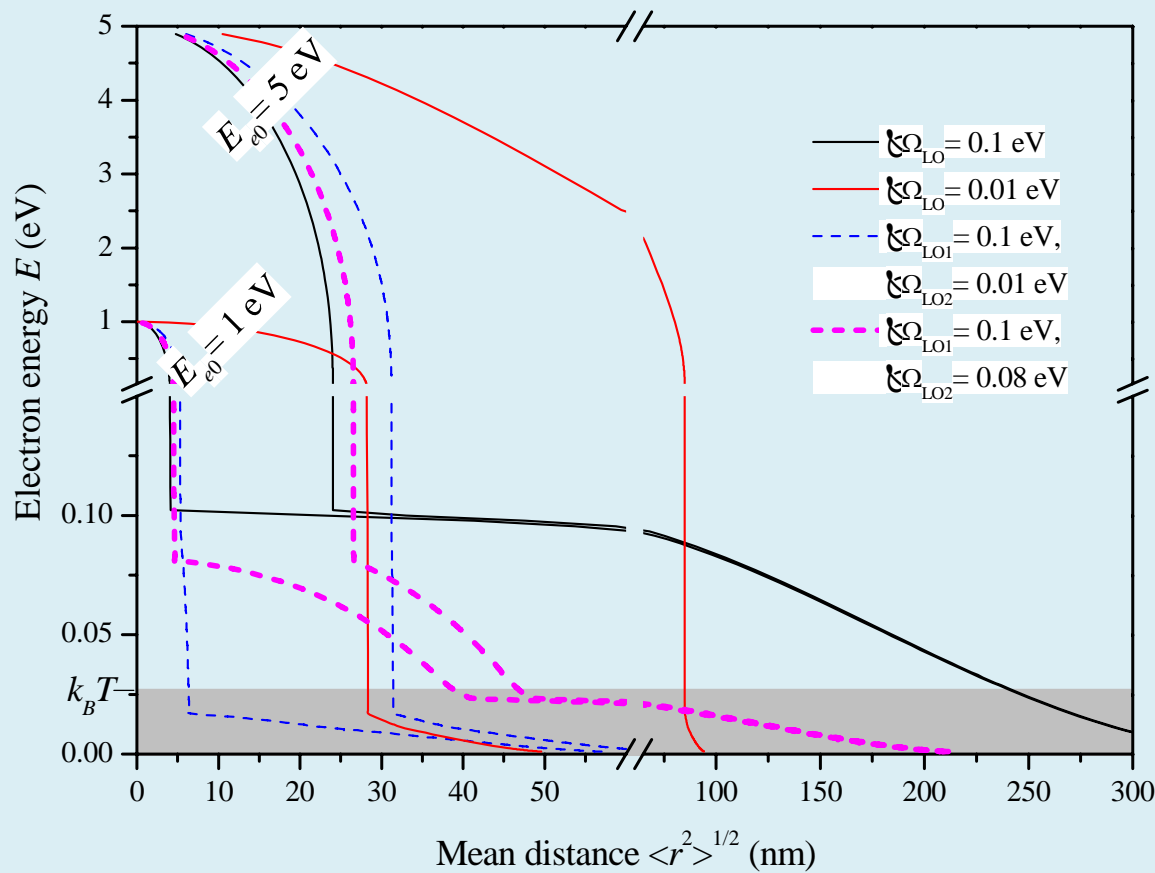


- Few LO branches (N atoms/cell  $\rightarrow$  (N-1) PLO) (Both spatial diffusion and relaxation are due to LO phonons)









# Outline

- Spatial scales for processes in scintillators
- Nanoparticles as scintillators
- Cascade, thermalization and recombination
- Different types of mobilities
- Thermalization length for different types of crystals
- **Interconnection of cascade, thermalization and recombination stages in binary iodides**
- Why cascade is so effective in CsI?
- Thermalization length and impurities
- Concluding remarks

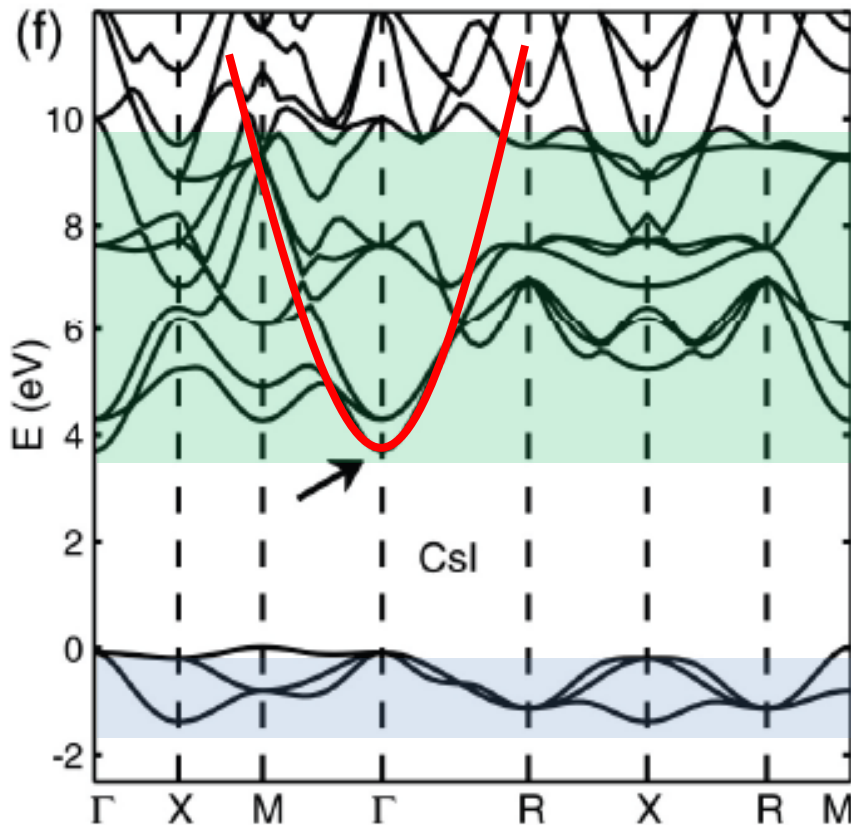


# Starting states for thermalization

$$(E_{\text{kin}} < E_{\text{g}})$$

## Band structure calculations

from W. Setyawan, R. M. Gaume et al. *IEEE TNS*, 2009



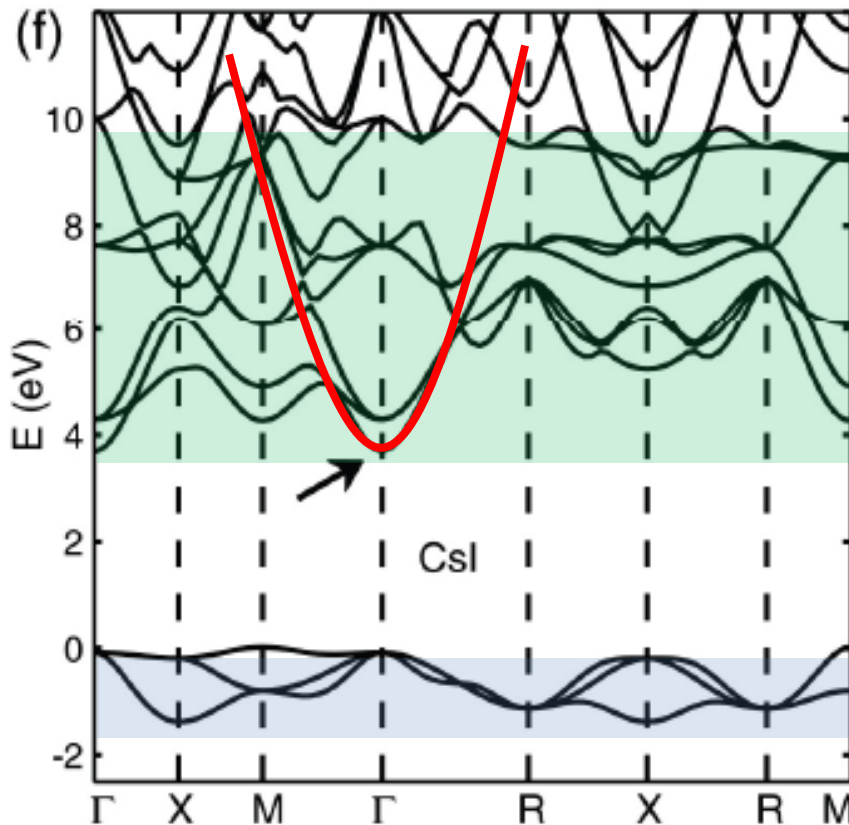
e-e passive region in CB after all e-e scattering events is filled mostly in low energy part

# Starting states for thermalization

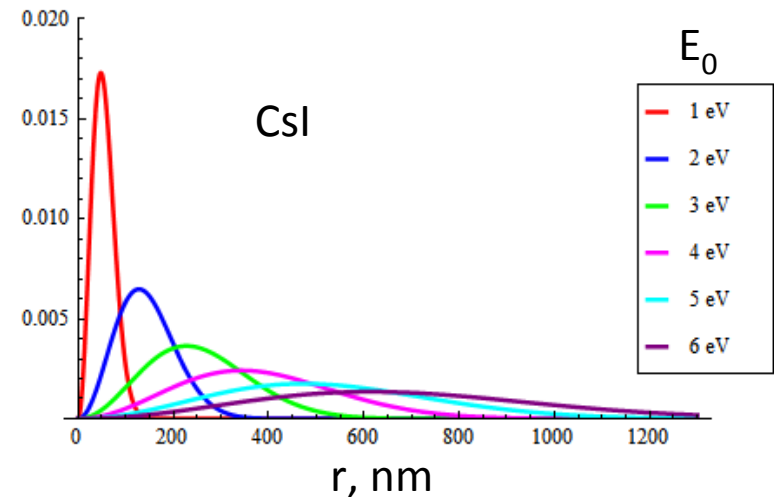
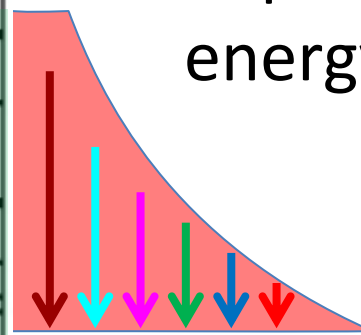
$$(E_{\text{kin}} < E_{\text{g}})$$

## Band structure calculations

from W. Setyawan, R. M. Gaume et al. *IEEE TNS*, 2009

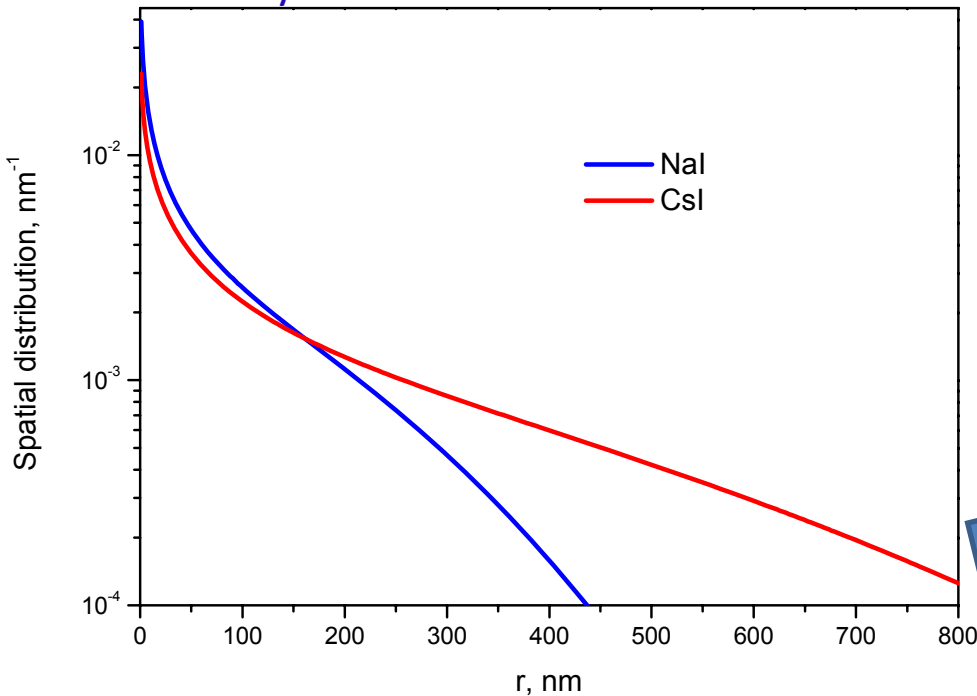


Thermalization length depends on kinetic energy as  $(E_{\text{kin}})^{3/2}$

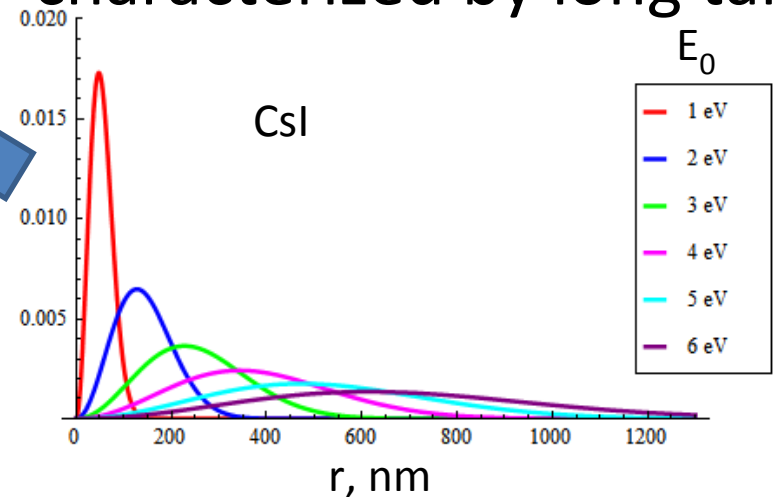


# Spatial distribution of thermalized electrons

Analytical estimation

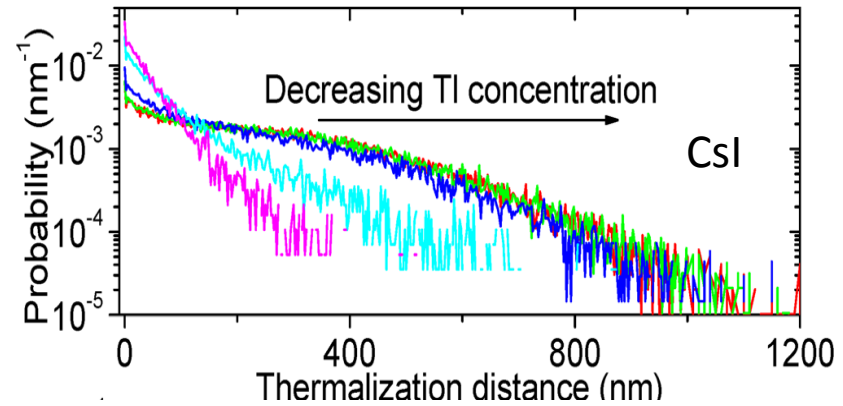
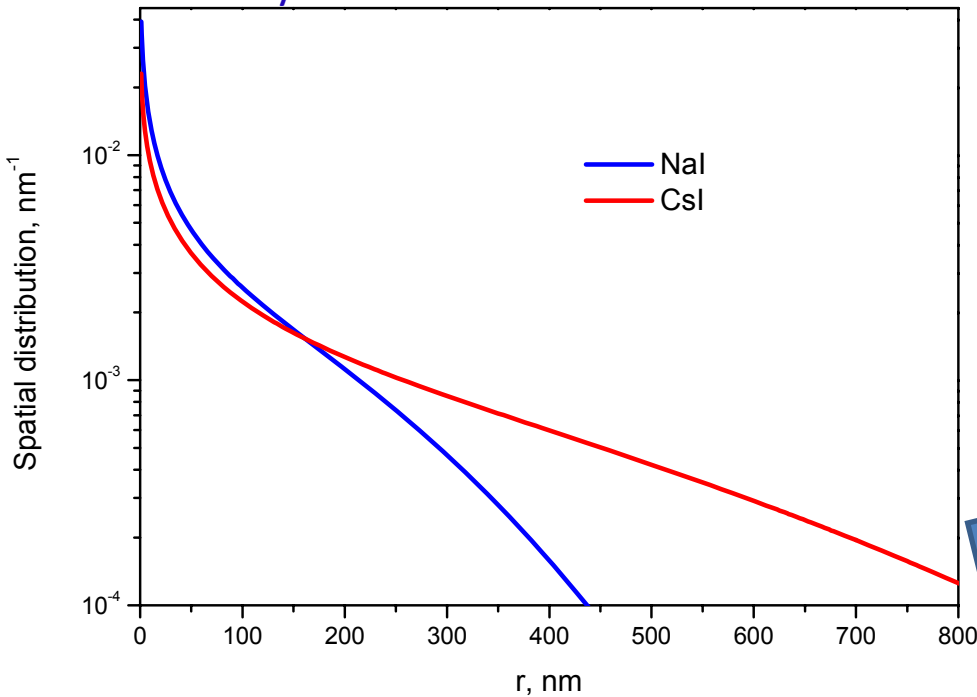


The resulting spatial distribution of excitations after thermalization is non-Gaussian and is characterized by long tail



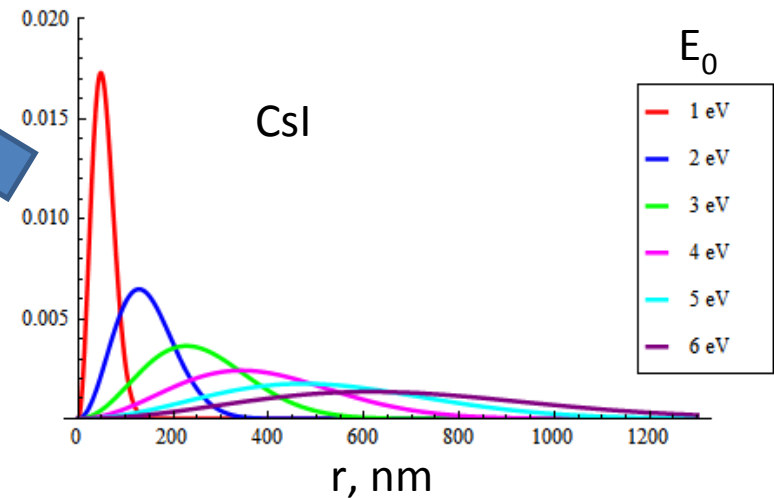
# Spatial distribution of thermalized electrons

Analytical estimation



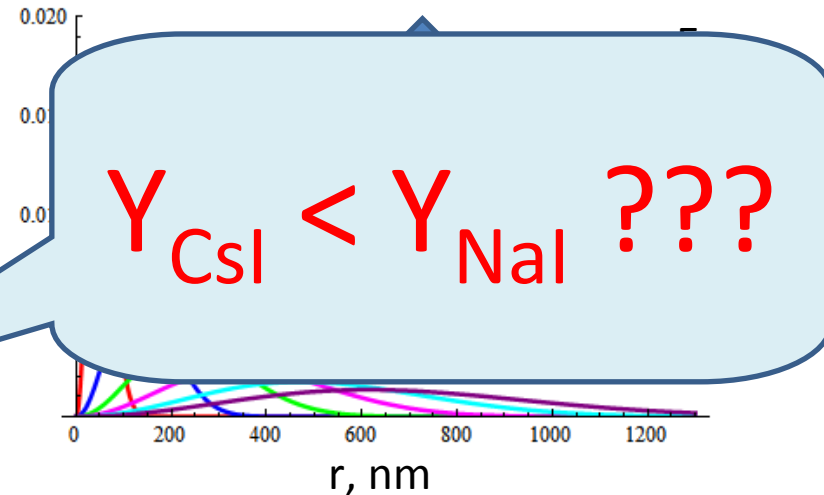
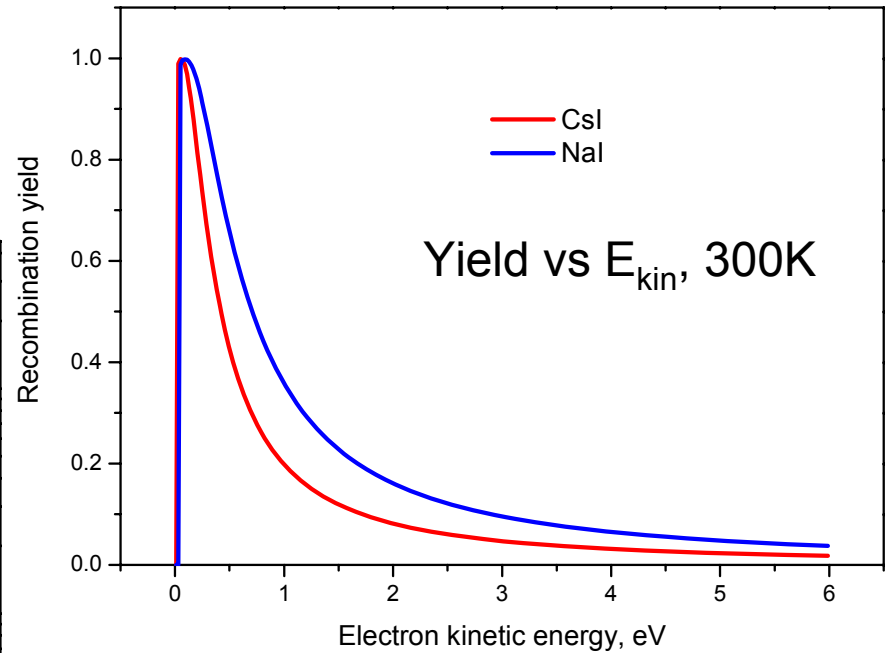
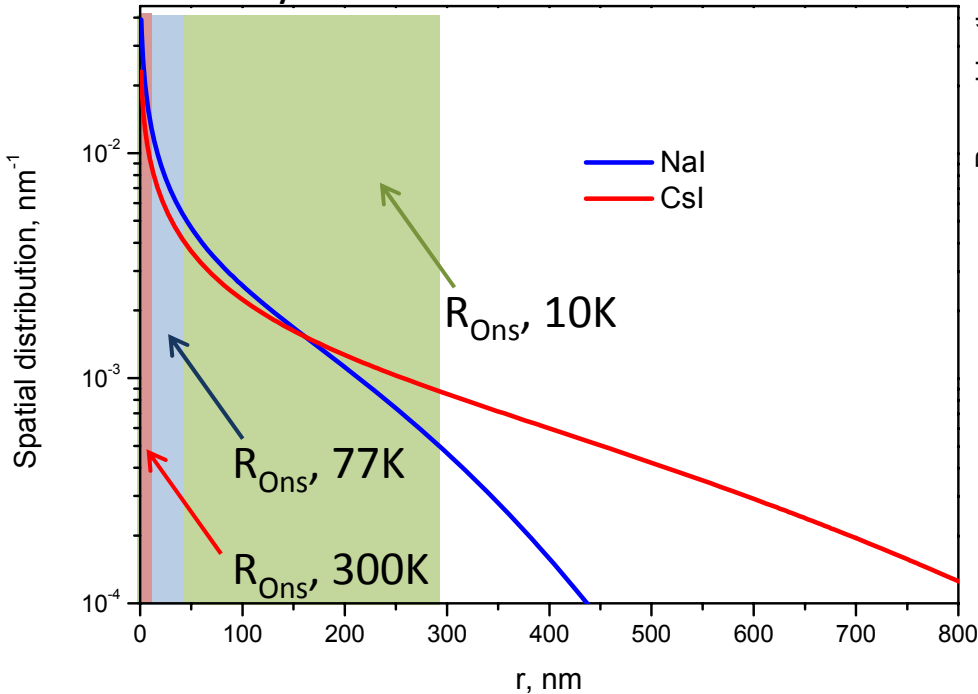
Computer simulation of electron thermalization in CsI and CsI(Tl),

Z. Wang, Y. Xie, B. D. Cannon et al. 2011



# Spatial distribution of thermalized electrons

Analytical estimation



|     | $R_{Ons}, 300K$ | Yield, 300K | Yield, 77K |
|-----|-----------------|-------------|------------|
| CsI | 9.87 nm         | 0.24        | 0.44       |
| NaI | 9.05 nm         | 0.34        | 0.58       |

# Outline

- Spatial scales for processes in scintillators
- Nanoparticles as scintillators
- Cascade, thermalization and recombination
- Different types of mobilities
- Thermalization length for different types of crystals
- Interconnection of cascade, thermalization and recombination stages in binary iodides
- **Why cascade is so effective in CsI?**
- Thermalization length and impurities
- Concluding remarks

# Transitions from 5pCs core levels

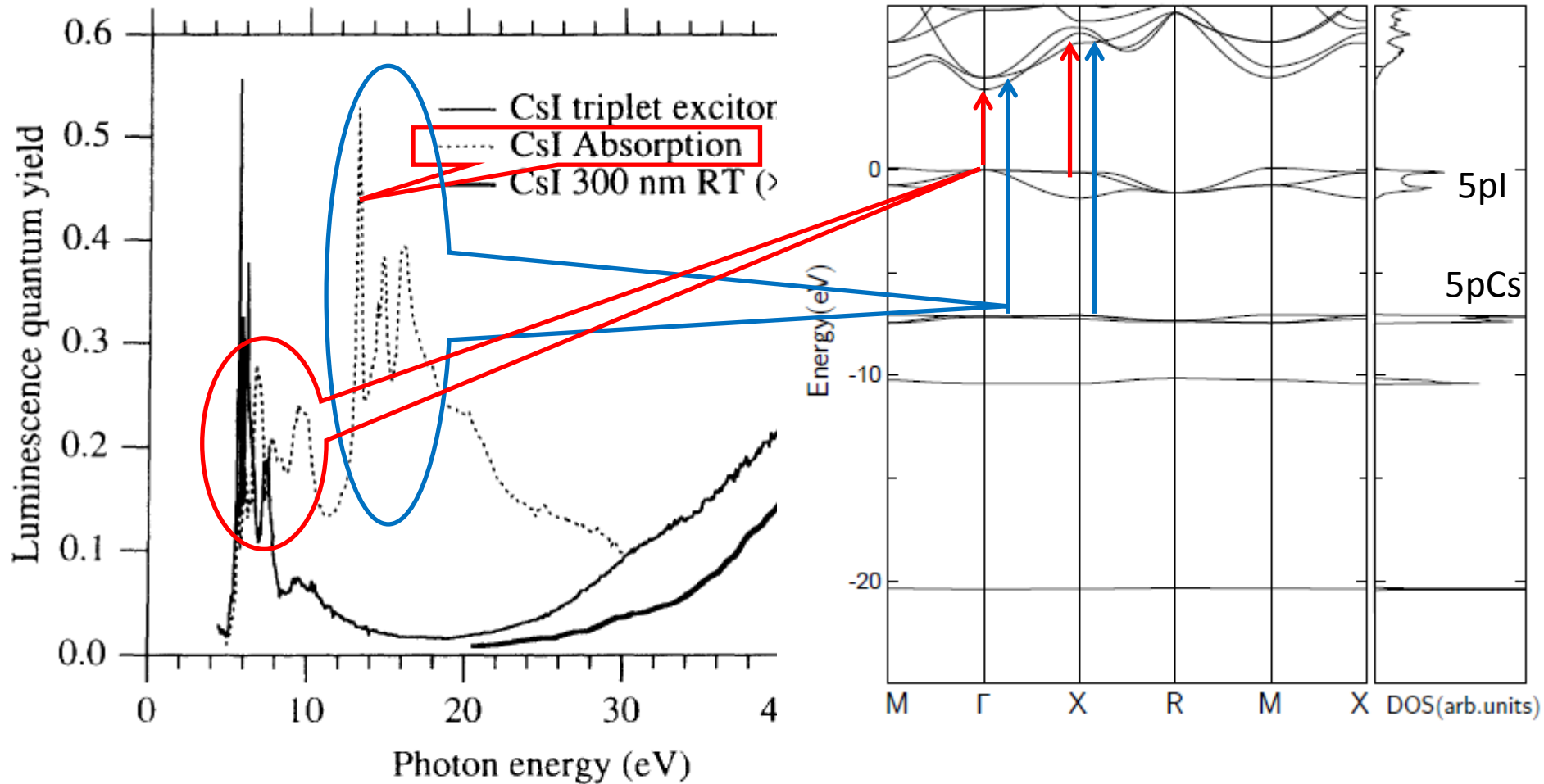
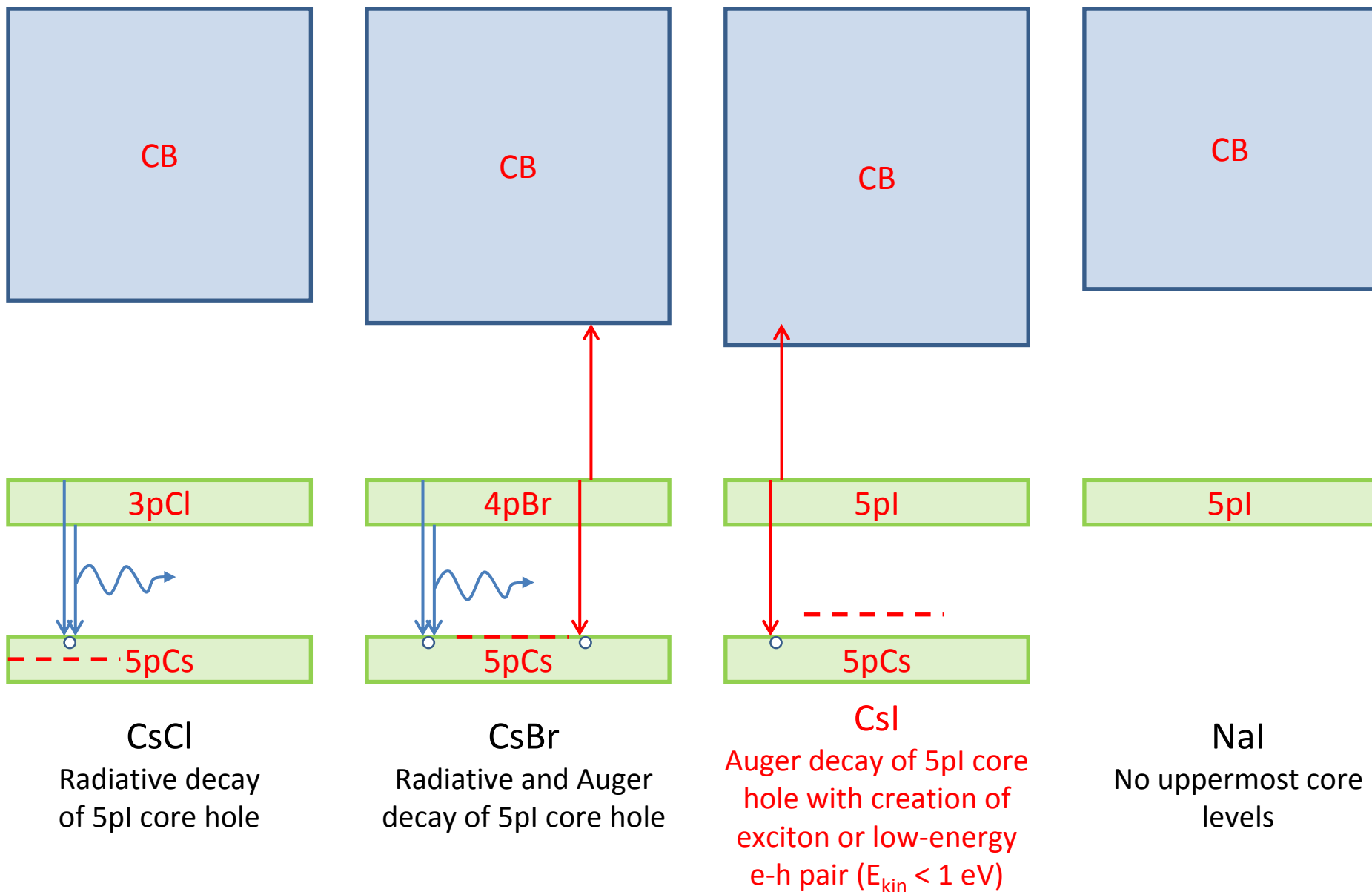


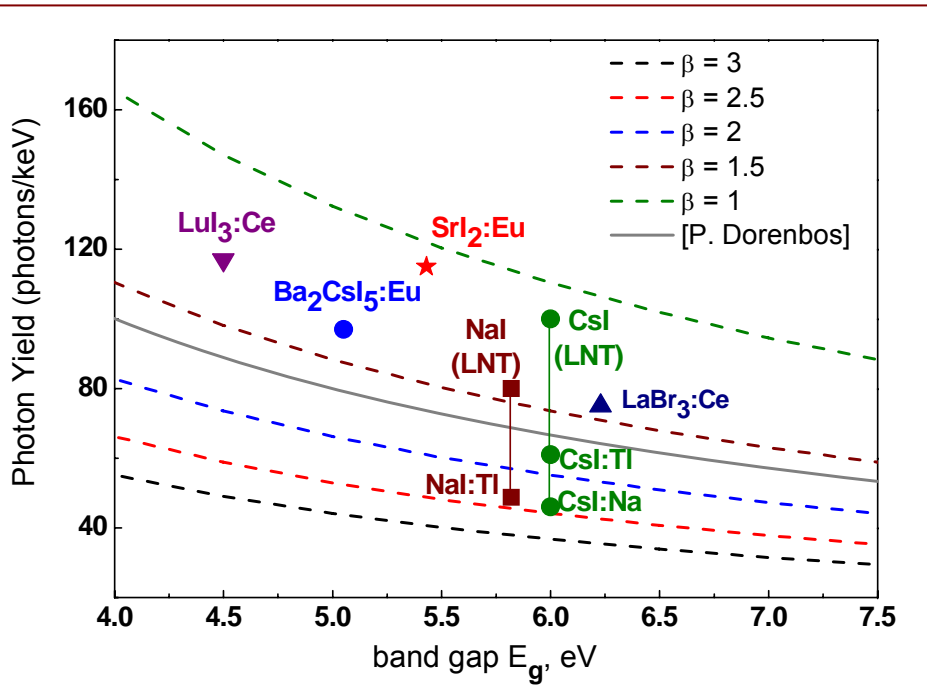
FIG. 2. Excitation spectra of CsI luminescence: the FIL (300 K) (thick) and of triplet exciton (100 K) (thin) compared with CsI absorption (dashed).

# From core-valence transitions to Auger process in cesium halides

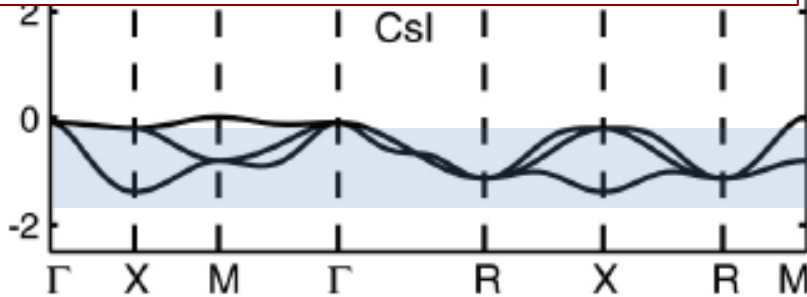
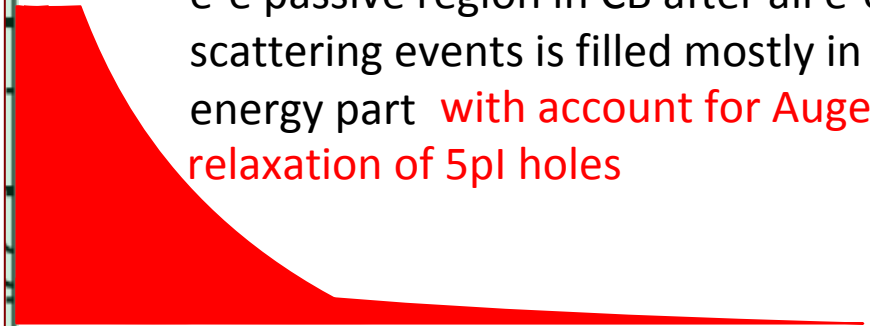




# Starting states for thermalization ( $E_{\text{kin}} < E_g$ )



e-e passive region in CB after all e-e scattering events is filled mostly in low energy part with account for Auger relaxation of 5p1 holes



Estimation of  $\beta$  decreases significantly!  
Creation of each 5p1 hole with threshold energy 13 eV produces 2 e-h pairs, one electron and both holes of which has low kinetic energy!

# Outline

- Spatial scales for processes in scintillators
- Nanoparticles as scintillators
- Cascade, thermalization and recombination
- Different types of mobilities
- Thermalization length for different types of crystals
- Interconnection of cascade, thermalization and recombination stages in binary iodides
- Why cascade is so effective in CsI?
- **Thermalization length and impurities**
- Concluding remarks

# Elastic scattering on impurities and carriers

$$\frac{1}{\tau} = \nu \sigma N = \sqrt{\frac{2E}{m^*}} \sigma N$$

Charged impurities/carriers: Conwell & Weisskopf (Phys. Rev. 77, 388-390, 1950)

$$\sigma_c^{CW} = 2\pi \left( \frac{Ze^2}{4\pi\epsilon_0\epsilon_{st}2E} \right)^2 \ln \left( 1 + 4 \left( \frac{E}{E_m} \right)^2 \right), \quad E_m = \frac{Ze^2}{4\pi\epsilon_0\epsilon_{st}r_m}, \quad r_m = \frac{1}{2}n_c^{-1/3}$$

$$\sigma_c^{CW} = \frac{1}{2}\pi R_{Ons}^2 \left( \frac{k_B T}{E} \right)^2 \ln \left( 1 + \left( \frac{E}{k_B T x_m} \right)^2 \right), \quad x_m = R_{Ons} n_c^{1/3}$$

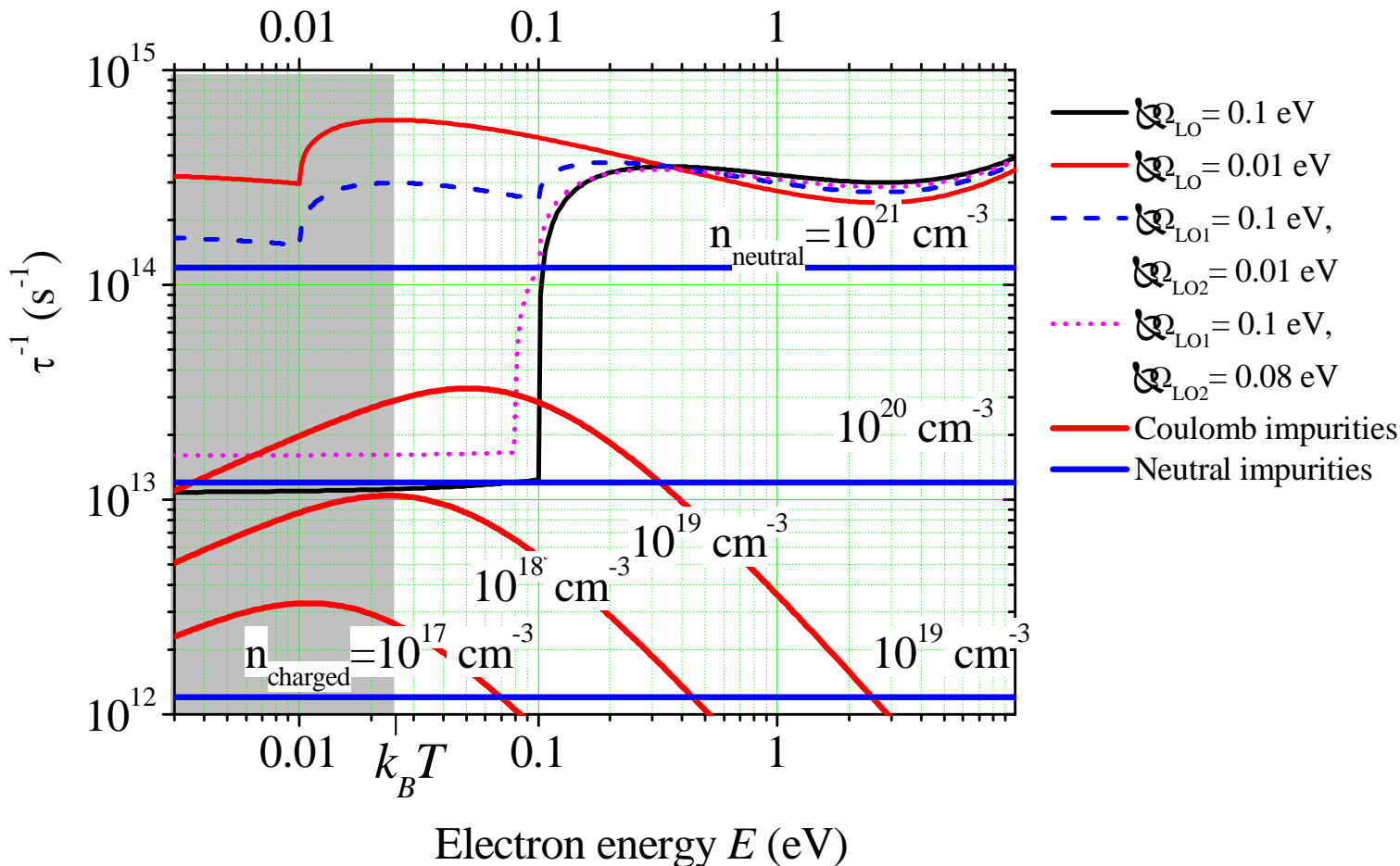
$$\frac{1}{\tau} = \sqrt{\frac{2k_B T}{m^*}} \frac{1}{2} \pi R_{Ons}^2 \left( \frac{k_B T}{E} \right)^{3/2} \ln \left( 1 + \left( \frac{E}{k_B T x_m} \right)^2 \right) n_c = 1.5 \times 10^{-5} \left( \frac{k_B T}{E} \right)^{3/2} \ln \left( 1 + \left( \frac{E}{k_B T x_m} \right)^2 \right) n_c [\text{cm}^{-3}] \frac{1}{\text{s}}$$

Neutral impurities

$$\sigma \approx 20 \frac{ka^*}{k^2}, \quad k = \frac{1}{\hbar} \sqrt{2m^*E}, \quad a^* - \text{impurity Bohr radius}$$

$$\sigma \approx \frac{20a^*\hbar}{\sqrt{2m^*E}}, \quad \frac{1}{\tau} = \frac{20a^*\hbar}{m^*} n = 1.2 \times 10^{-7} n [\text{cm}^{-3}] \frac{1}{\text{s}} = 1.2 \times 10^{13} n [\text{mol.}\%] \frac{1}{\text{s}} \quad (a^* = 1\text{nm}, m^* = m_e)$$

# Elastic scattering on impurities and carriers



Scattering on impurities is the limiting factor for thermalization length only for crystals with high LO phonon energies in LO-passive region for high concentrations of neutral ( $>0.5\%$ ) impurities and for high concentration of carriers ( $>10^{18} \text{ cm}^{-1}$ )

# Conclusions

The development of comprehensive model of scintillator based on multi-particle consideration of multi-scale evolution of strongly non-equilibrium excited region on the basis of deep directional experimental investigations allows to

- Make a progress in fundamental physics
- Obtain new results in applied physics – e.g. by justification that mixed crystals is a way to improve scintillator properties
- Be useful in pragmatic sense, because it is a background for new material development (industrial applications)

Thank you for your attention  
and cooperation!